

La physique aujourd'hui

des manuels scolaires

jusqu'aux labos de recherche

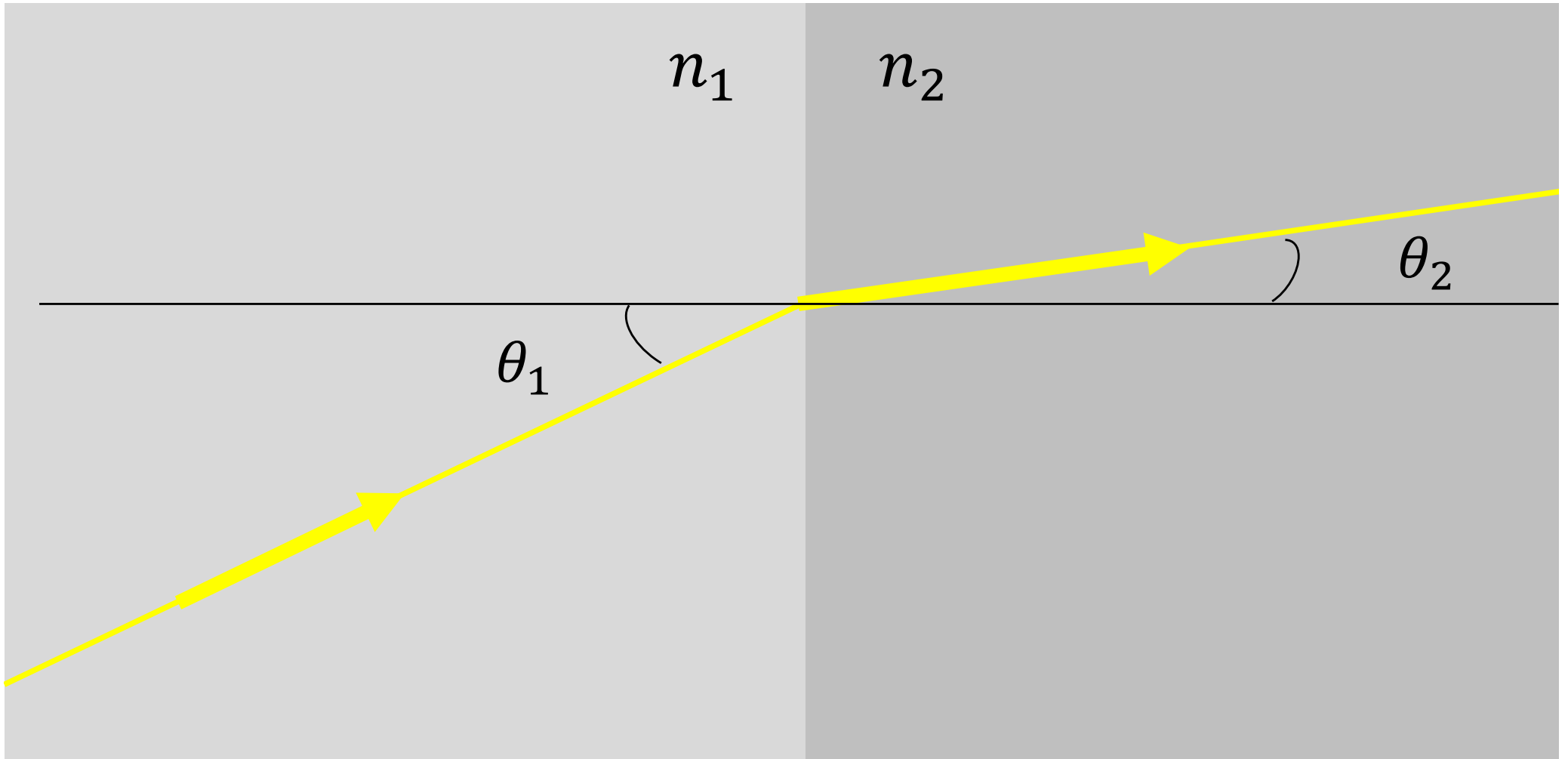
L'optique géométrique et les lois de Snell-Descartes

Julien Bobroff

julien.bobroff@u-psud.fr

la loi de refraction de Descartes

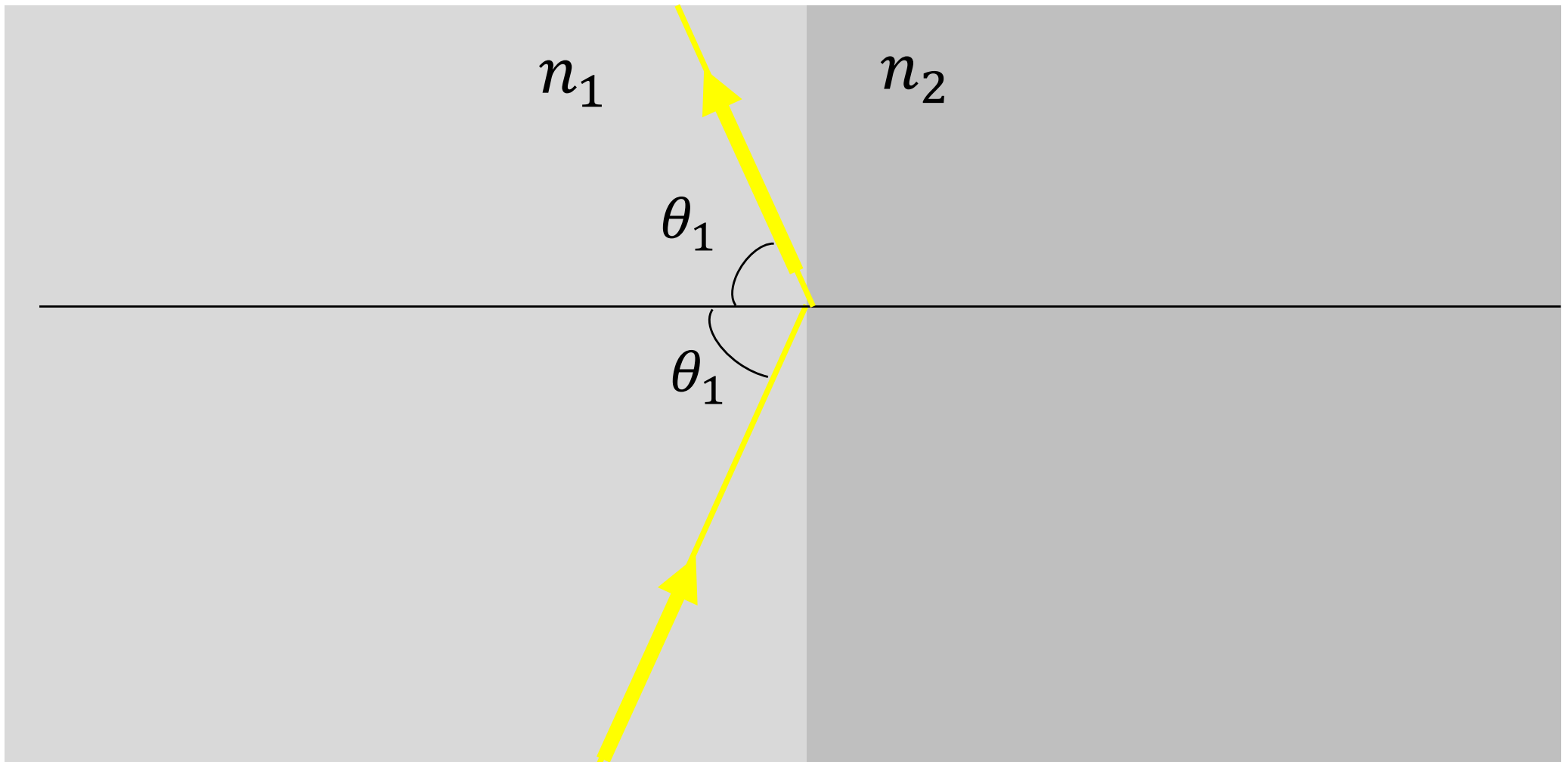
$$n_1 \sin \theta_1 = n_2 \sin \theta_2$$



la loi de refraction de Descartes

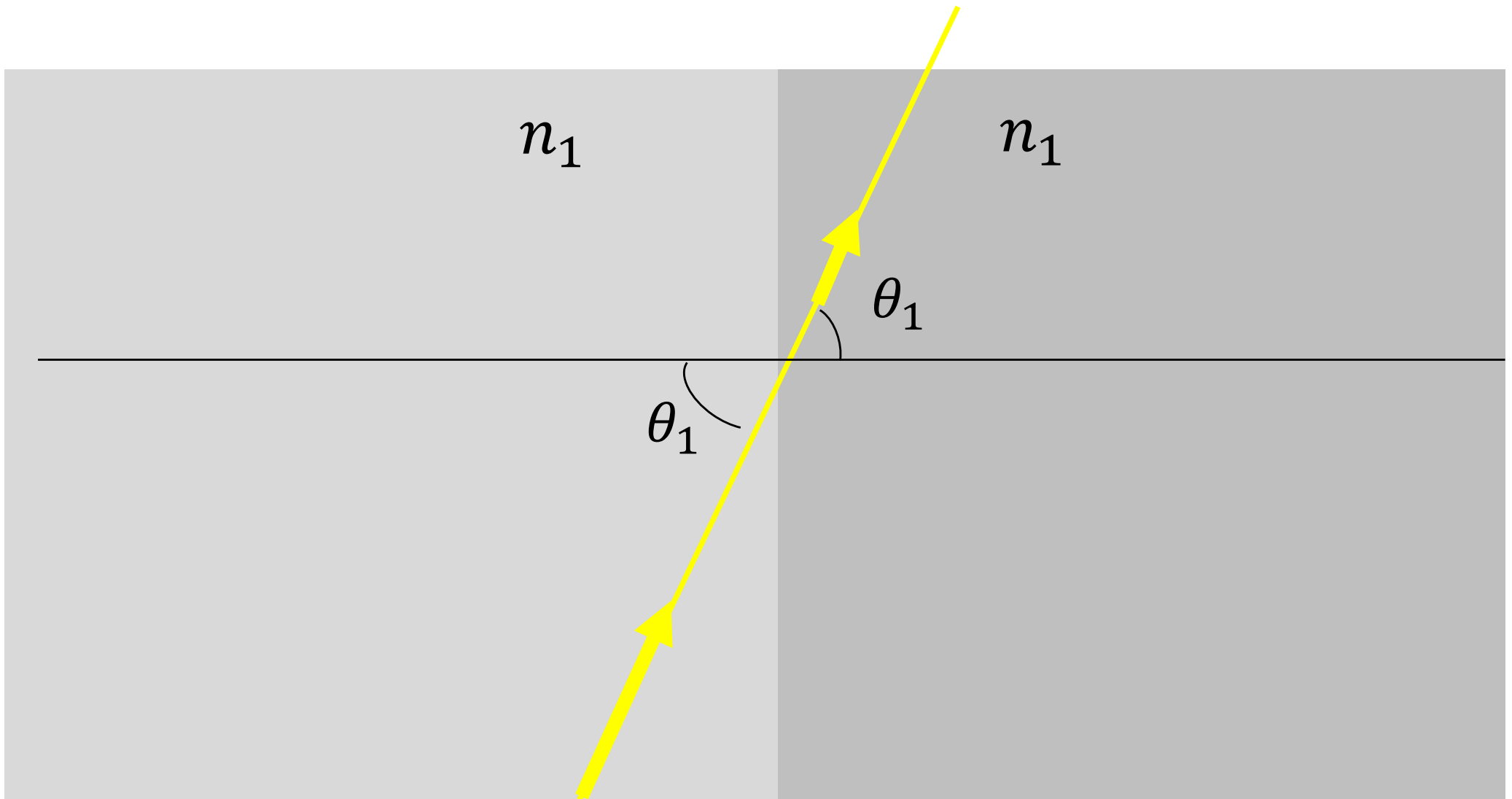
Si $n_1 > n_2$ et si $\frac{n_1}{n_2} \sin \theta_1 > 1$ alors reflexion totale

Donc réflexion totale au delà de $\theta_{lim} = \arcsin\left(\frac{n_2}{n_1}\right)$



la loi de refraction de Descartes

Si $n_1 = n_2$ alors pas d'effet



L'optique et les lois de Descartes

1. Visualiser les lois de Snell-Descartes en voyant la lumière se déplacer
2. Les métamatériaux
3. Les cristaux photoniques (si on a le temps)

L'optique et les lois de Descartes

I. Visualiser les lois de Snell-Descartes en voyant la lumière se déplacer

voir les lois de Descartes

au cours du temps :

difficile car dans le vide la lumière a

une vitesse $v = c = 3 \cdot 10^8$ m/s

dans la matière : $v = c / n$

LETTER

doi:10.1038/nature14005

Single-shot compressed ultrafast photography at one hundred billion frames per second

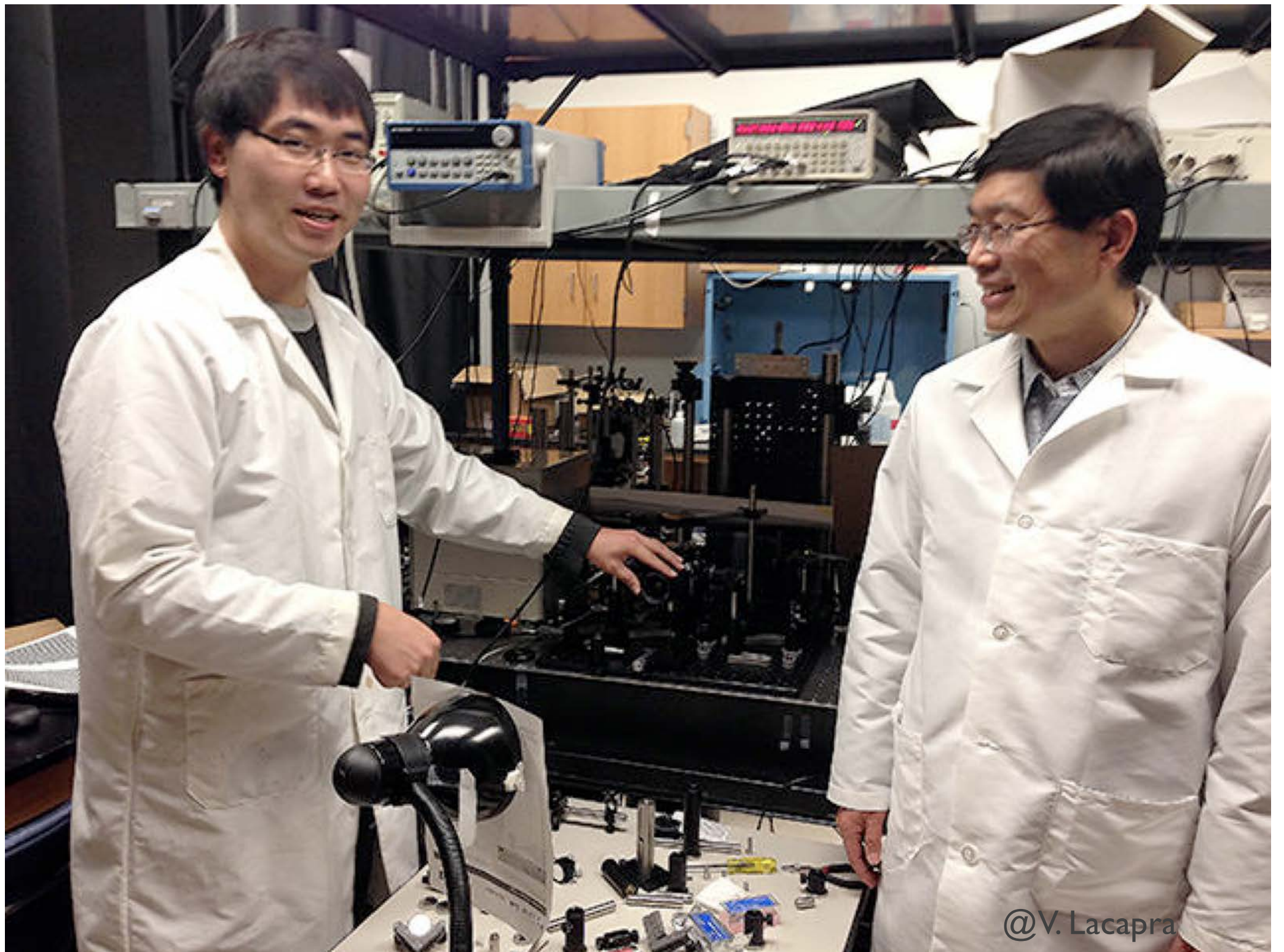
Liang Gao^{1*}, Jinyang Liang^{1*}, Chiye Li¹ & Lihong V. Wang¹

The capture of transient scenes at high imaging speed has been long sought by photographers^{1–4}, with early examples being the well known recording in 1878 of a horse in motion⁵ and the 1887 photograph of a supersonic bullet⁶. However, not until the late twentieth century were breakthroughs achieved in demonstrating ultrahigh-speed imaging (more than 10^5 frames per second)⁷. In particular, the introduction of electronic imaging sensors based on the charge-coupled device (CCD) or complementary metal-oxide-semiconductor (CMOS) technology revolutionized high-speed photography, enabling acquisition rates of up to 10^7 frames per second⁸. Despite these sensors' widespread impact, further increasing frame rates using CCD or CMOS technology is fundamentally limited by their on-chip storage and electronic readout speed⁹. Here we demonstrate a two-dimensional dynamic imaging technique, compressed ultrafast photography (CUP), which can capture non-repetitive time-evolving events at up to 10^{11} frames per second. Compared with existing ultrafast imaging techniques, CUP has the prominent advantage of measuring an x - y - t (x , y , spatial coordinates; t , time) scene with a single camera snapshot, thereby allowing observation of transient events with temporal reso-

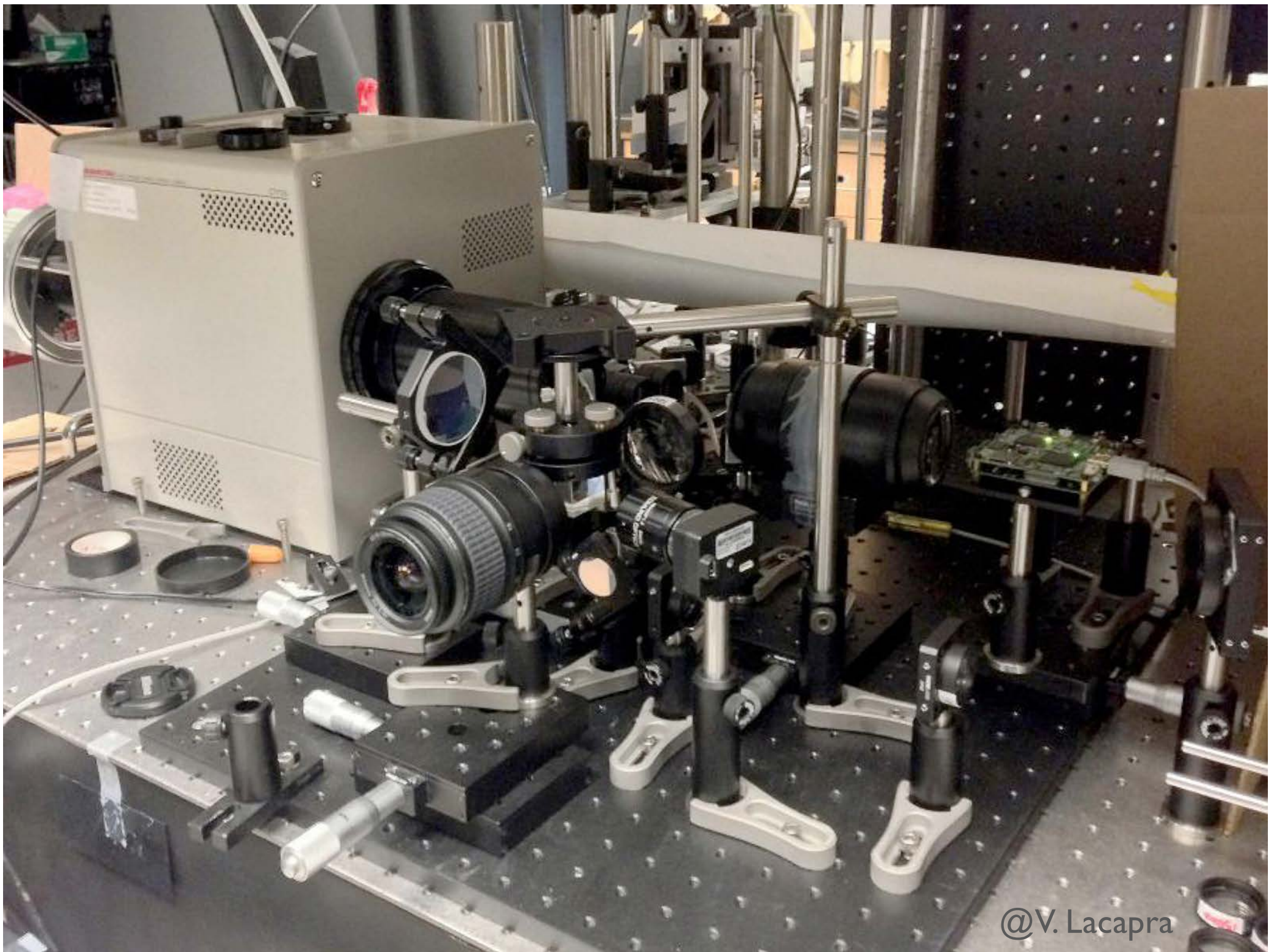
operation in the temporal domain, performed using a streak camera with a fully opened entrance slit. This encoded, sheared three-dimensional (3D) x , y , t scene is then measured by a 2D detector array, such as a CCD, with a single snapshot. The image reconstruction process follows a strategy similar to compressed-sensing-based image restoration^{15–19}—iteratively estimating a solution that minimizes an objective function.

By adding a digital micromirror device as the spatial encoding module and applying the CUP reconstruction algorithm, we transformed a conventional one-dimensional streak camera into a 2D ultrafast imaging device. The resultant system can capture a single, non-repetitive event at up to 100 billion frames per second with appreciable sequence depths (up to 350 frames per acquisition). Moreover, by using a dichroic mirror to separate signals into two colour channels, we expand CUP's functionality into the realm of four dimensional (4D) x , y , t , λ ultrafast imaging, maximizing the information content that we can simultaneously acquire from a single instrument (Methods).

CUP operates in two steps: image acquisition and image reconstruction. The image acquisition can be described by a forward model (Methods). The input image is encoded with a pseudo-random binary pattern

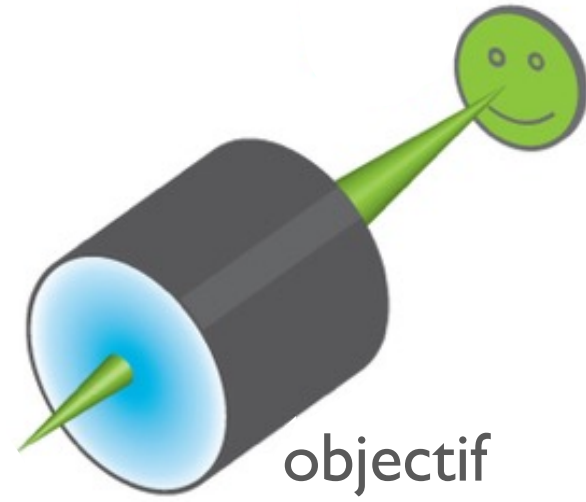


@V.Lacpra

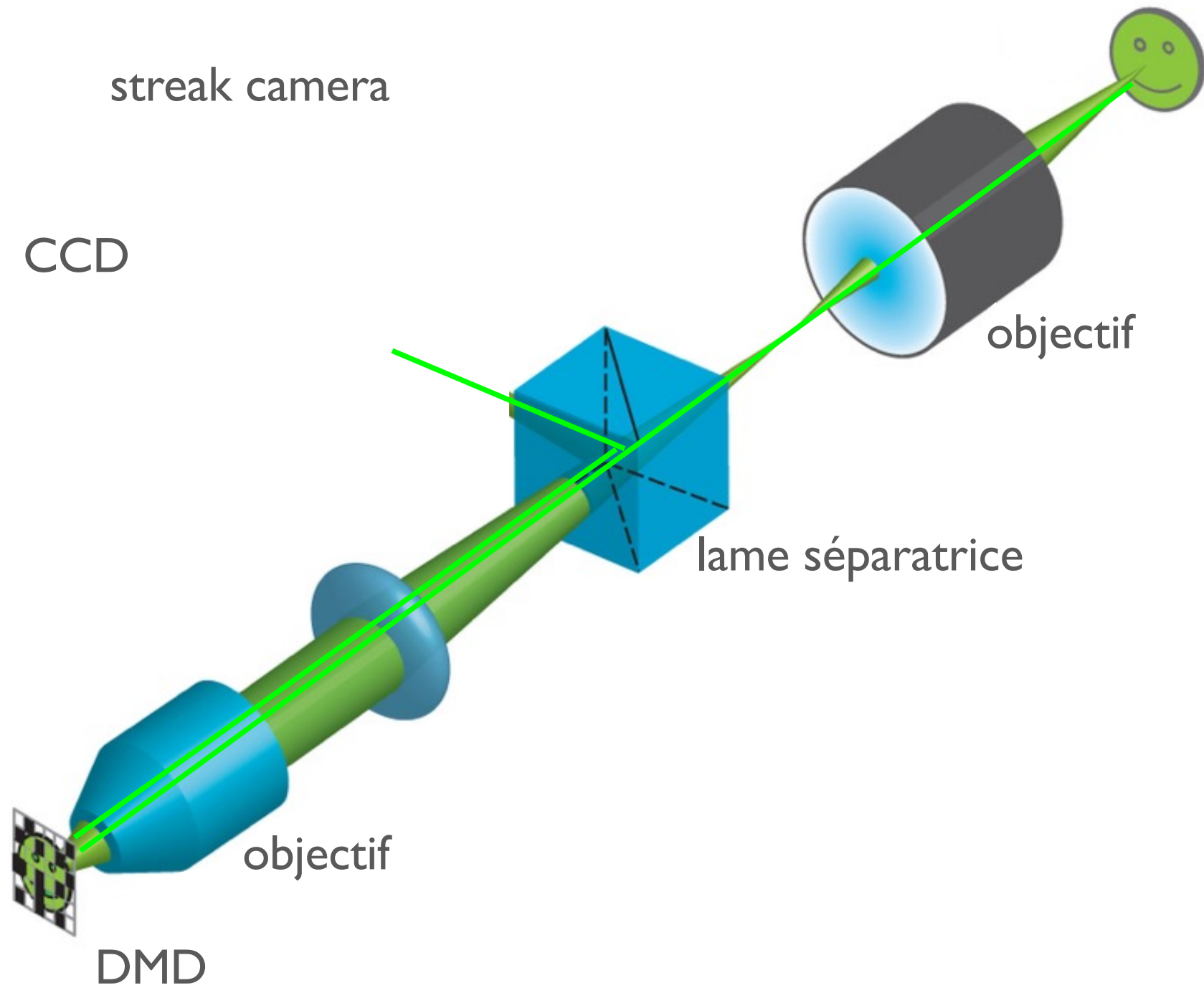


@V. Lacapra





objectif



streak camera

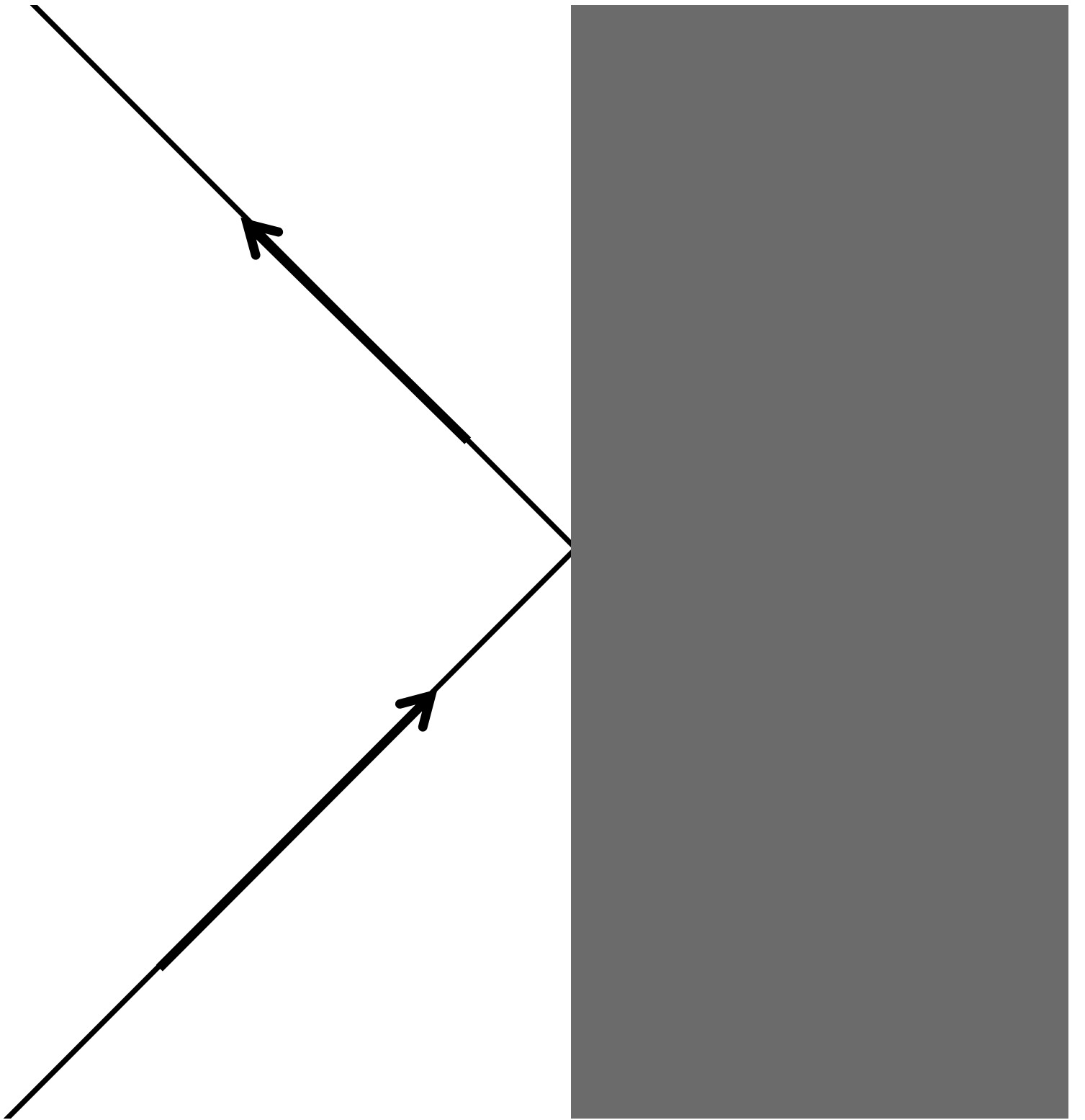
CCD

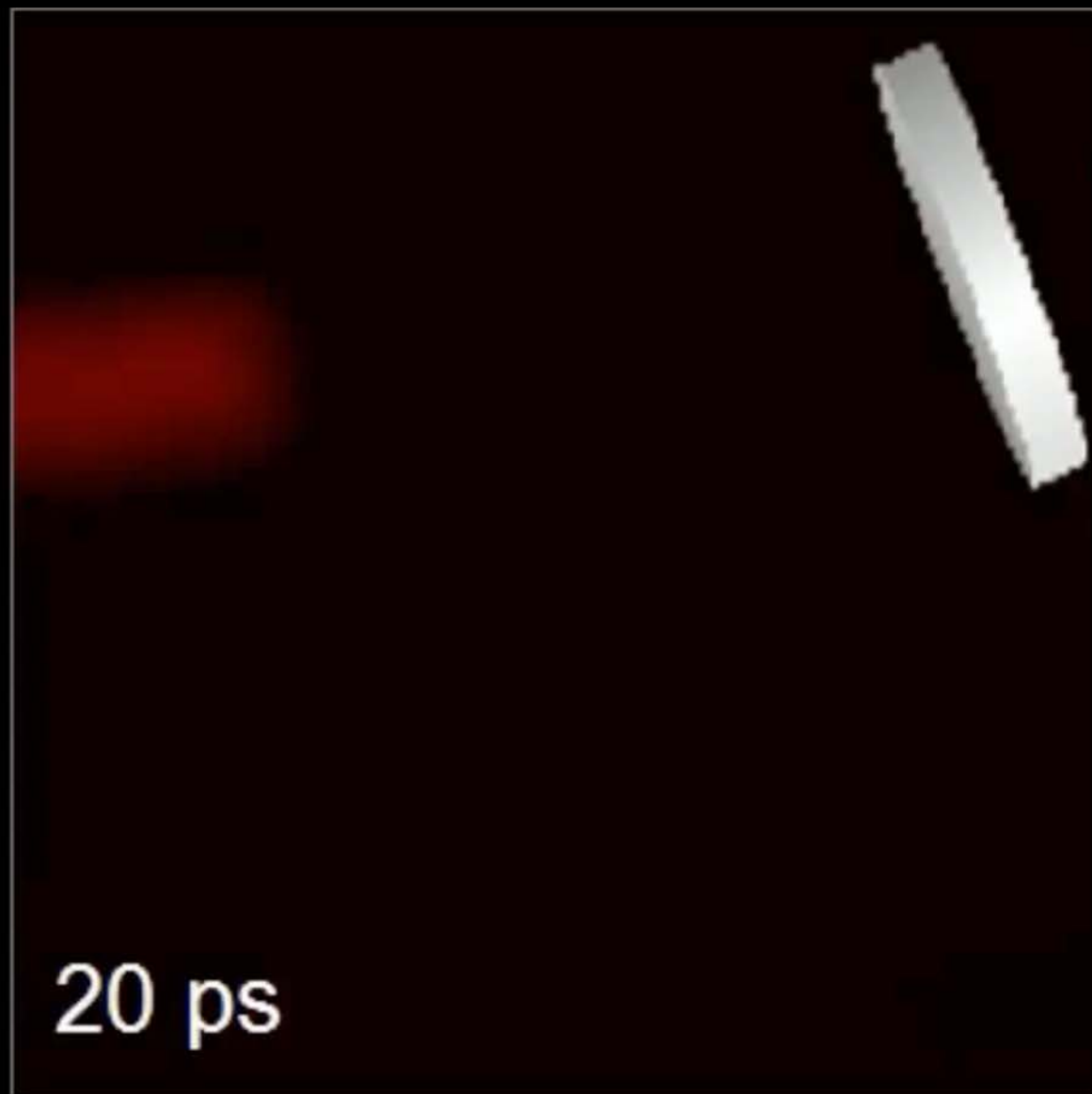
objectif

lame séparatrice

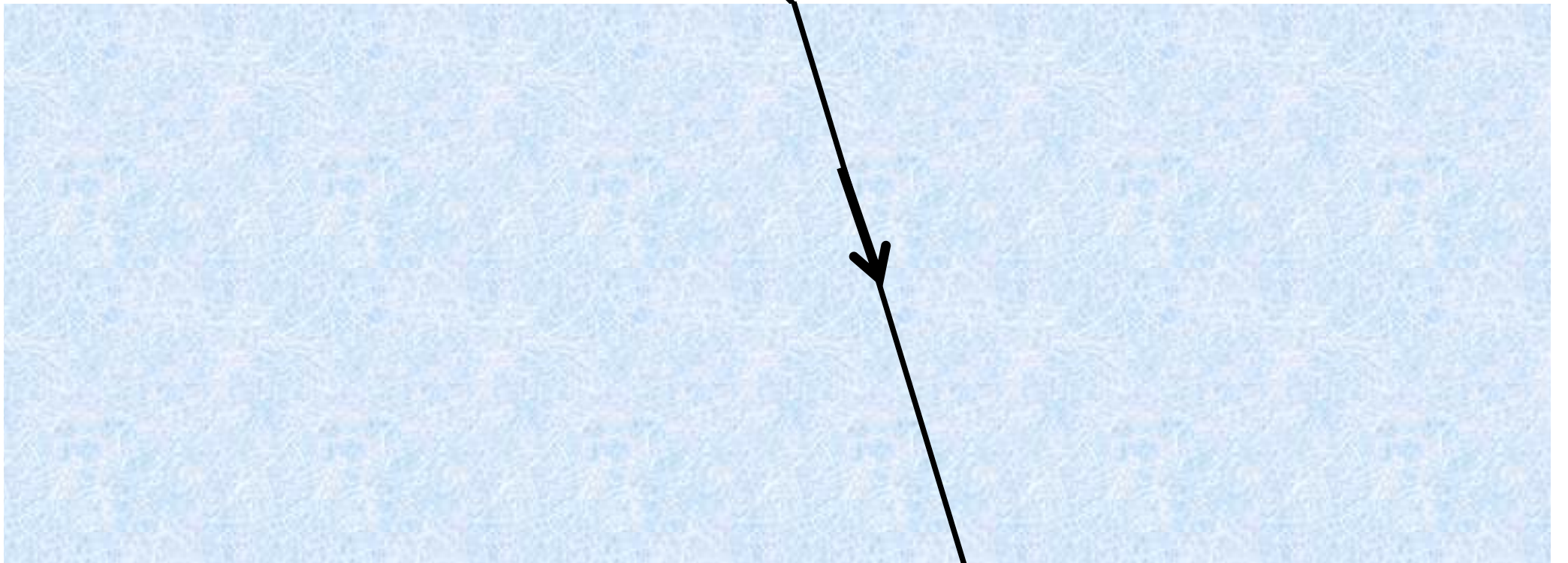
objectif

DMD





Deuxième loi de Snell-Descartes



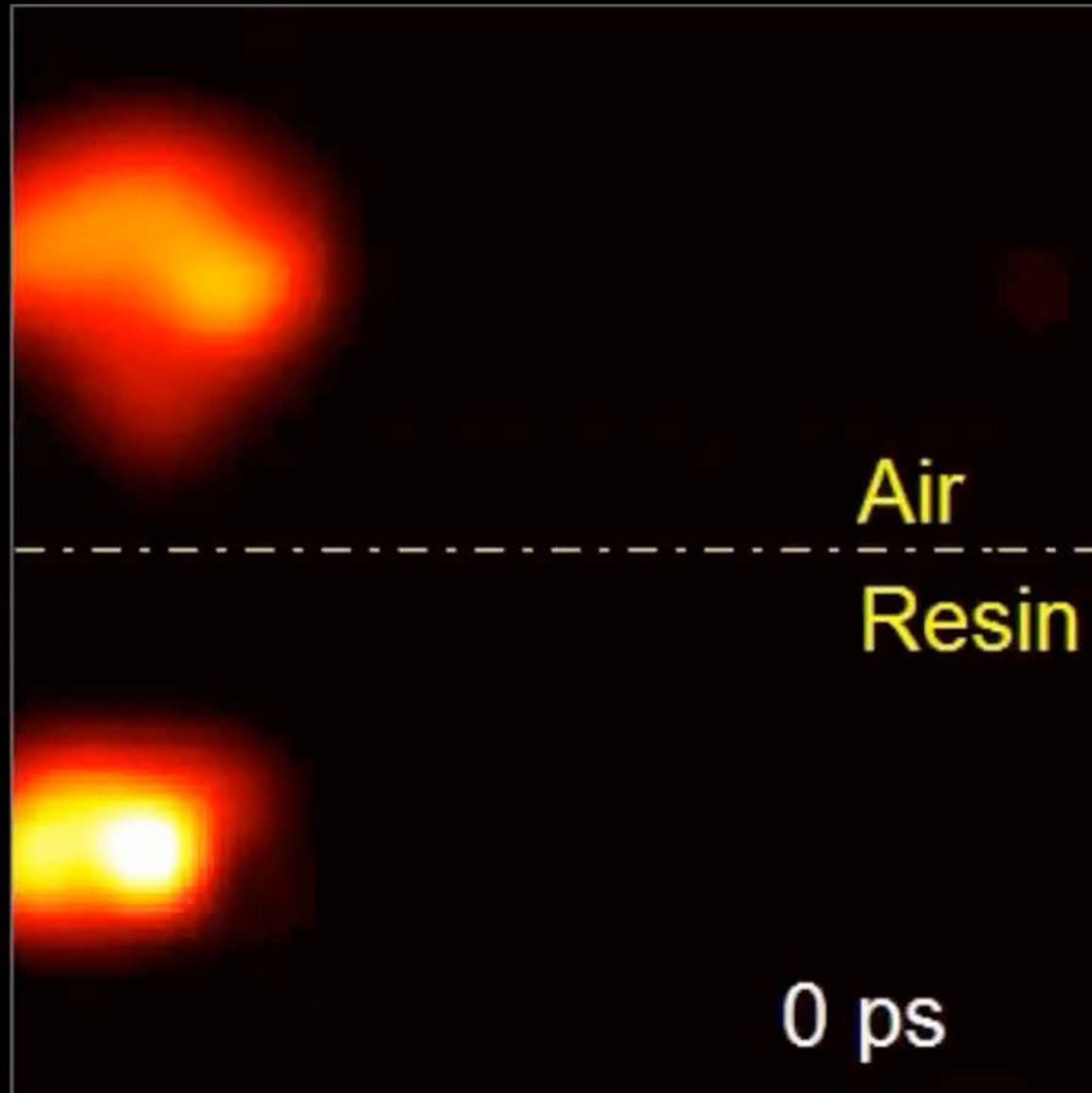


Air

Resin

20 ps

$$v = \frac{c}{n}$$



L'optique et les lois de Descartes

1. Visualiser les lois de Snell-Descartes en voyant la lumière se déplacer

2. Les métamatériaux

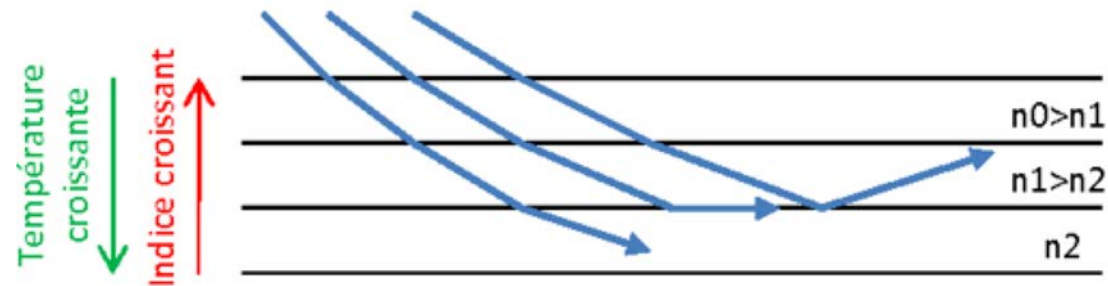
Les métamatériaux :
« tricher » avec les lois de la
réfraction

un exemple « naturel » où les lois de réfraction
provoquent des phénomènes curieux :
les mirages

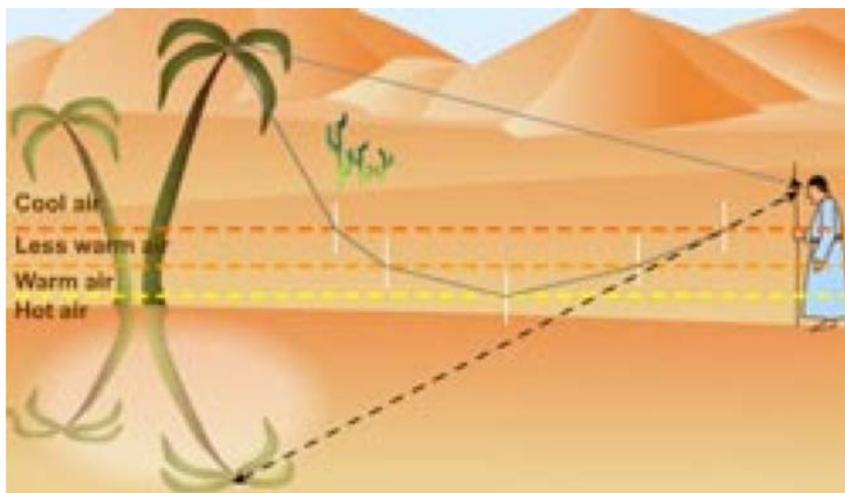


un exemple « naturel » où les lois de réfraction provoquent des phénomènes curieux : les mirages

→ variation de l'indice lié à la température de l'air

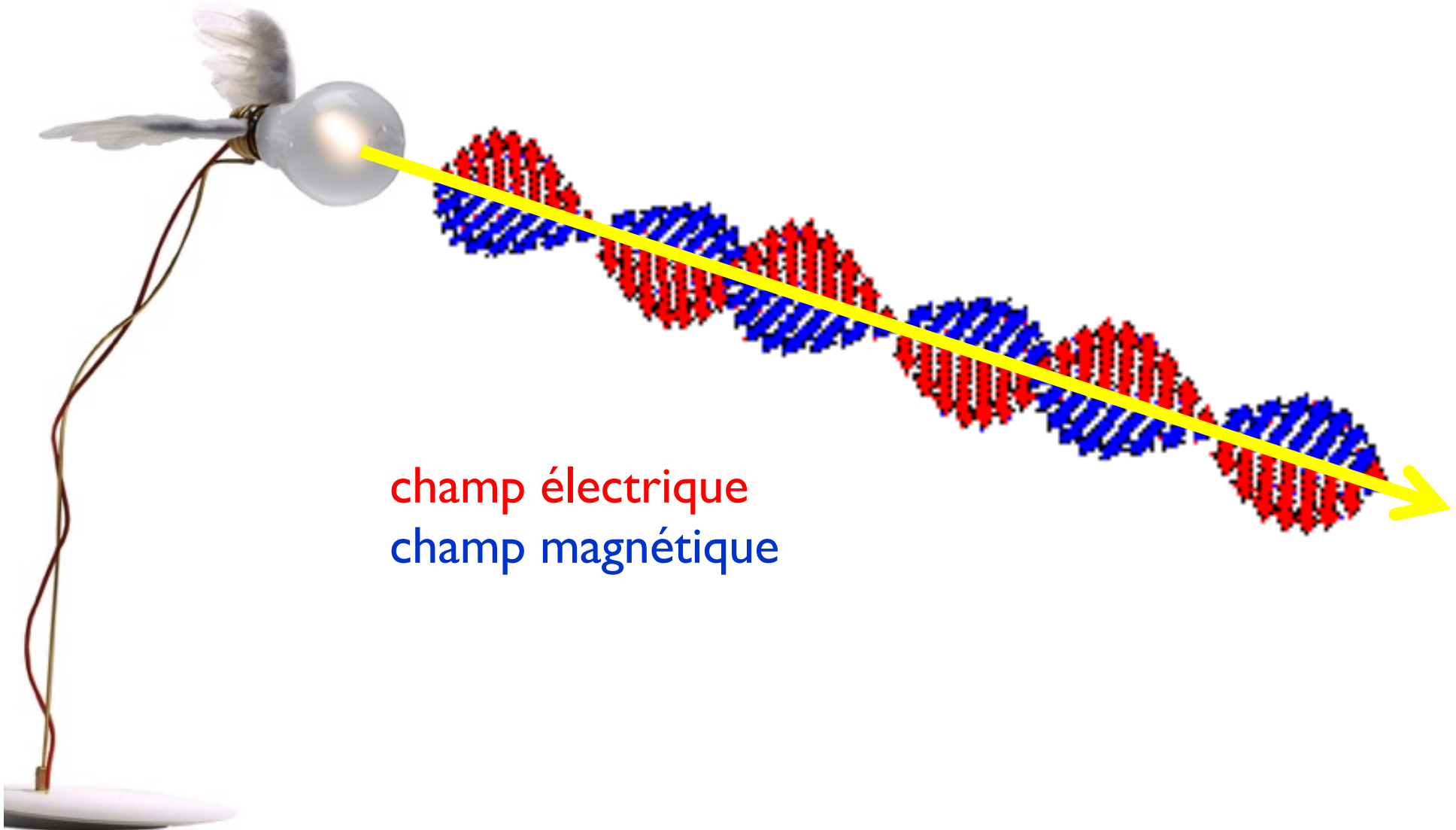


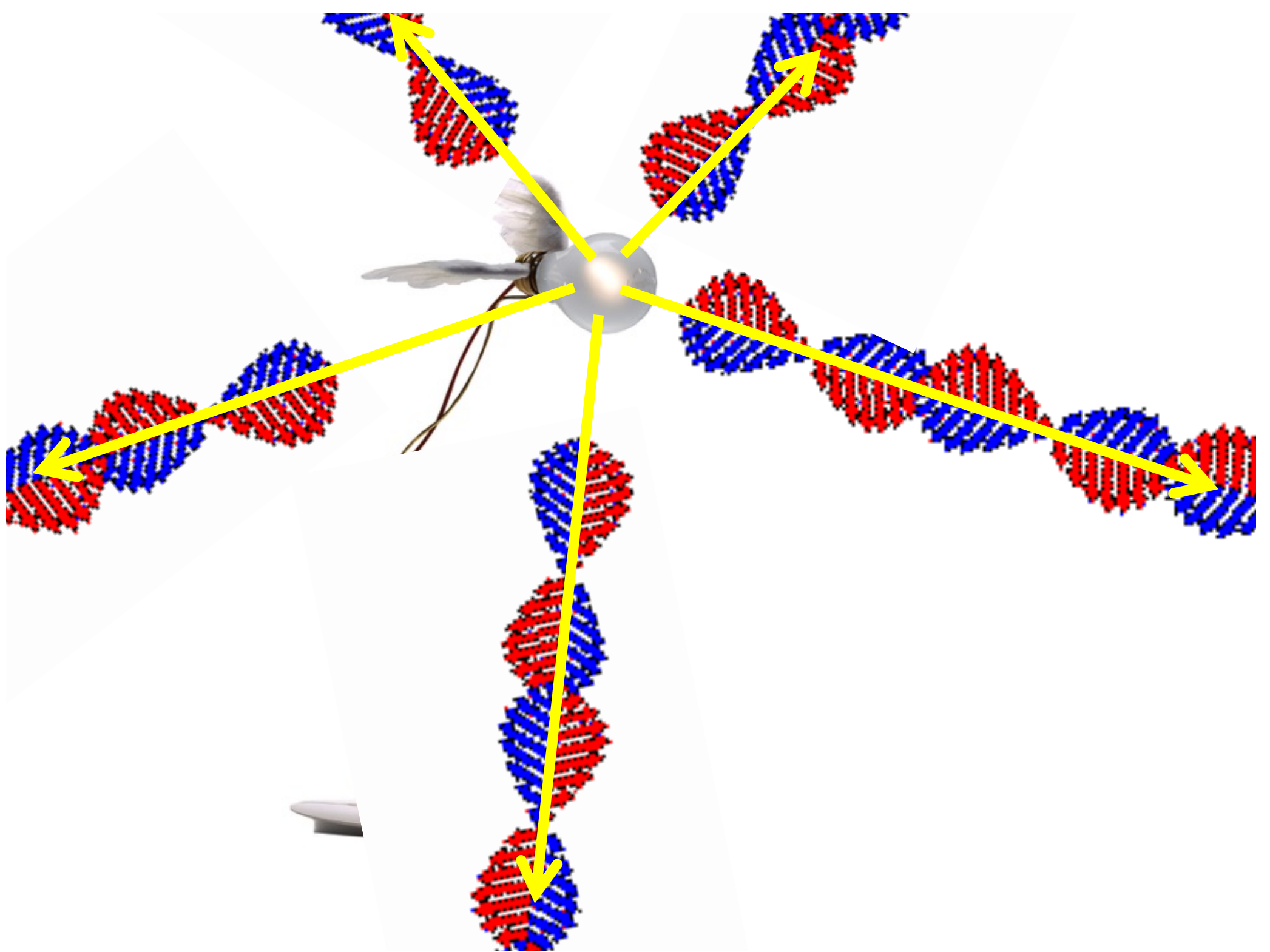
Courbure des rayons lumineux dans un milieu dit « stratifié », où la variation des indices de réfraction se fait de manière continue

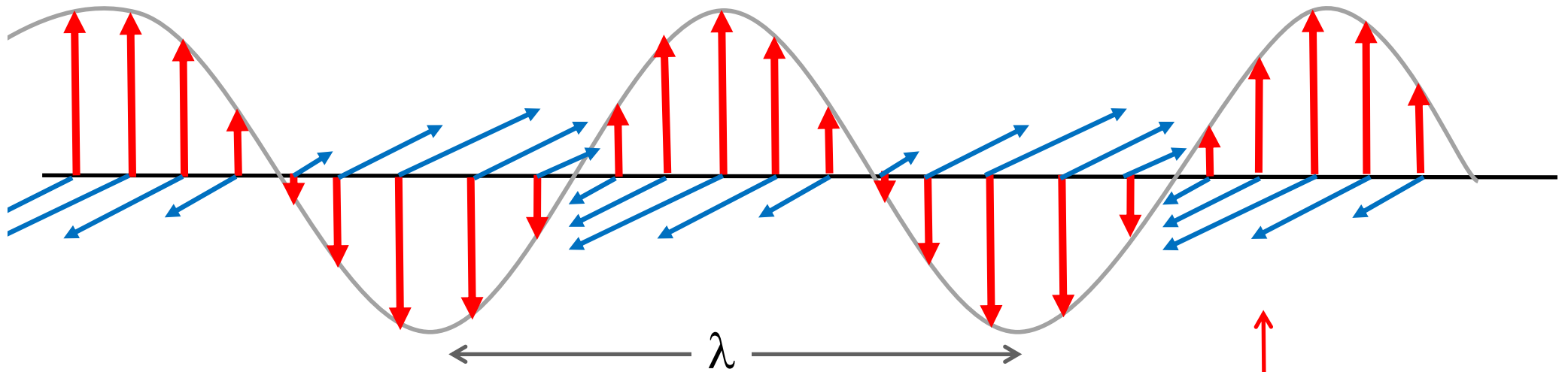


idée clé pour les métamatériaux :
agir sur l'indice de réfraction n
avec des petits composants électriques ou
magnétiques car la lumière est un champ
électromagnétique

La lumière est une onde électromagnétique







champ électrique
champ magnétique

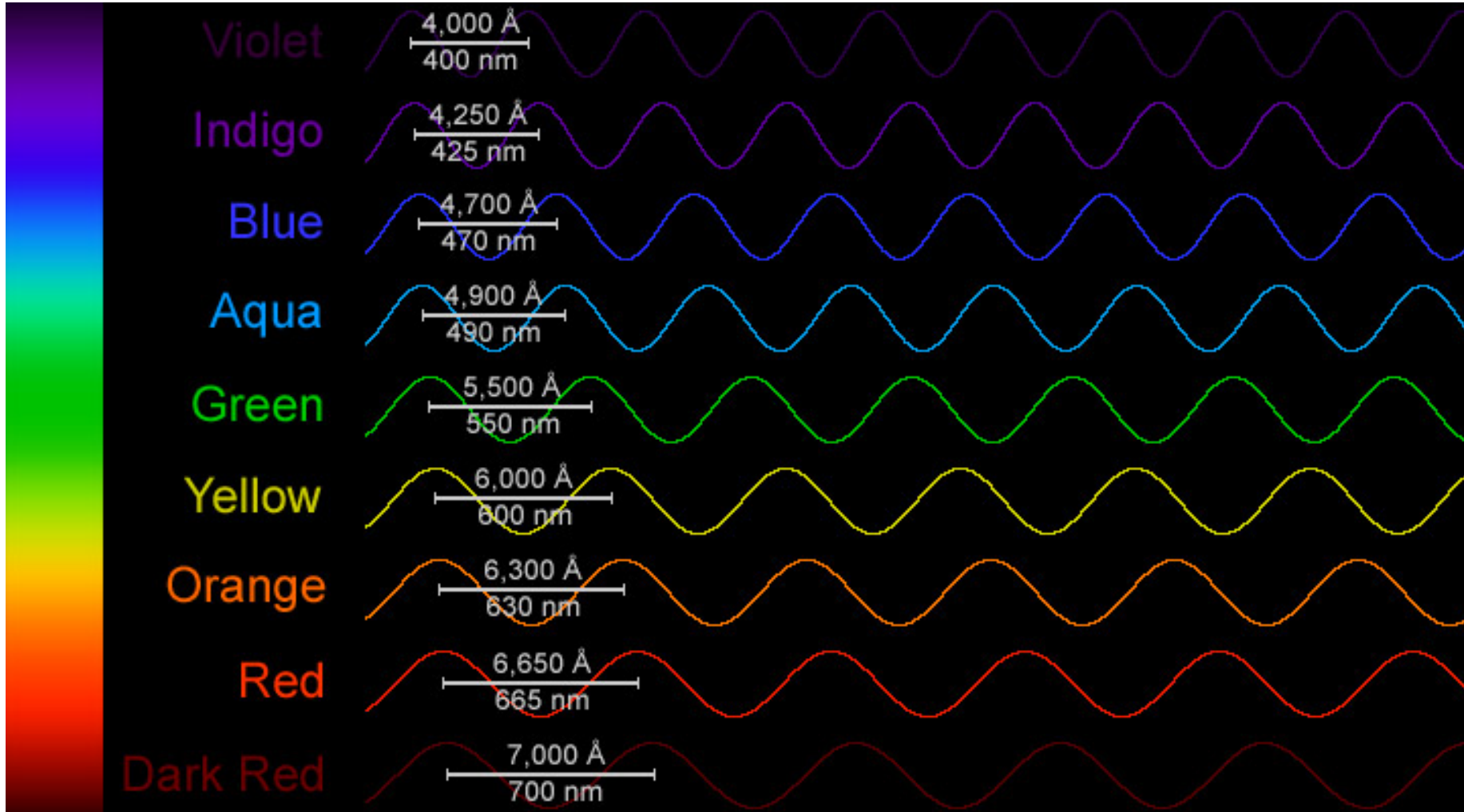
polarisation

longueur d'onde λ : longueur d'une oscillation (en mètres)

fréquence ν : nombre de fois que l'onde oscille par seconde (en Hertz)

polarisation : sens du champ

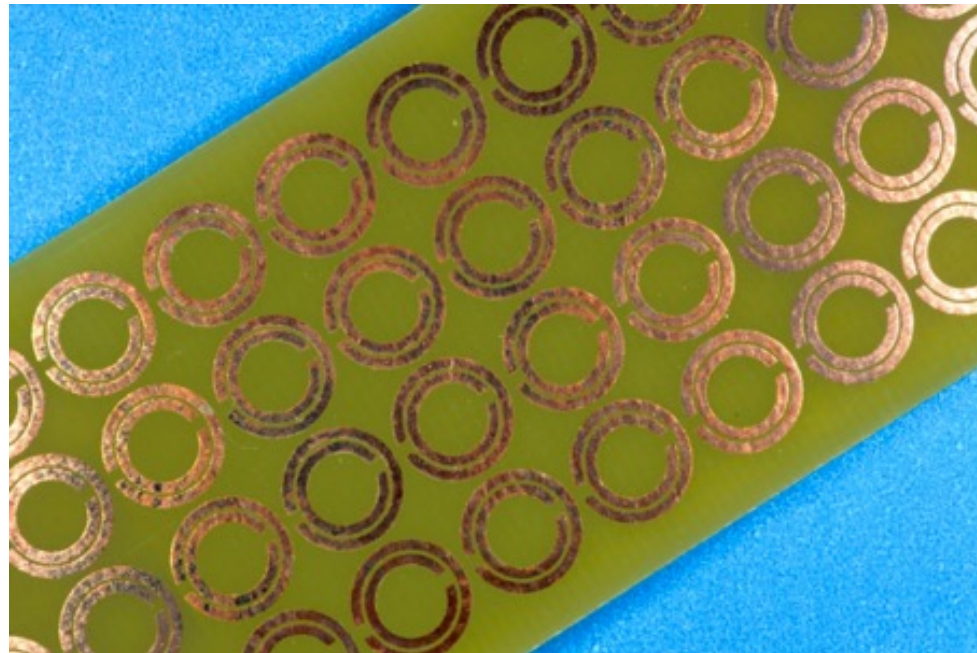
la longueur d'onde est la couleur



les métamatériaux : utiliser des structures qui agissent sur le champ électrique et magnétique à la place de la matière habituelle

concrètement :

des circuits résonants type RLC placés périodiquement à des tailles typiques de $\lambda/10$

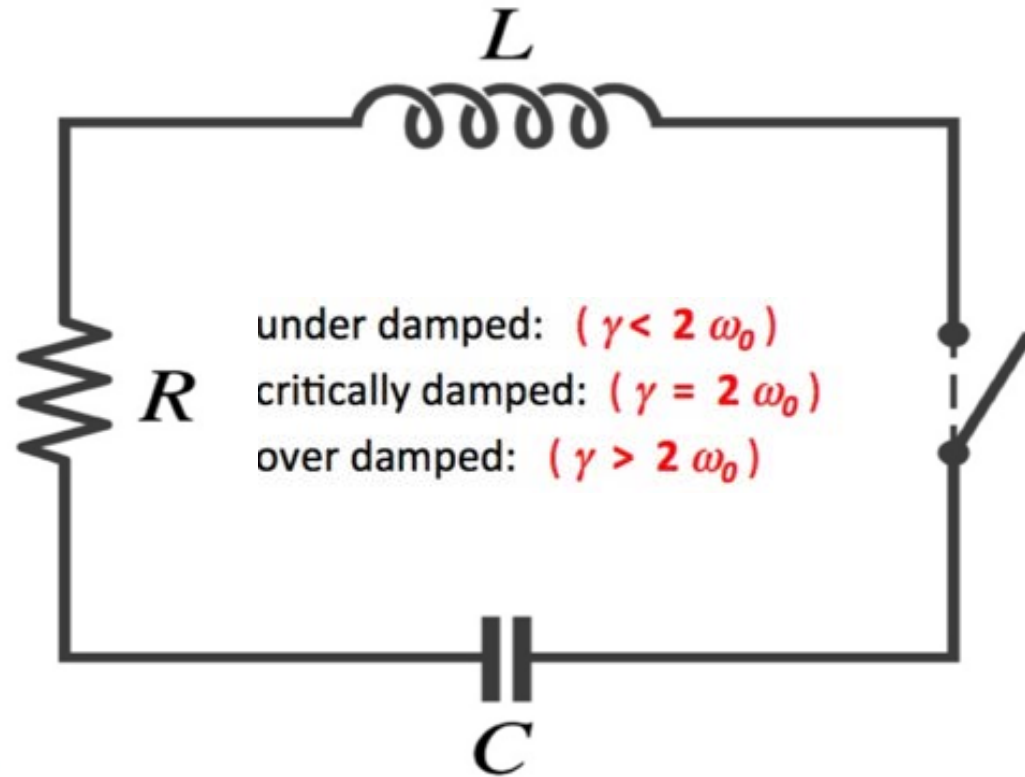


le premier métamatériau

D. R. Smith, W. J. Padilla, et al, Phys. Rev. Lett. 14, 234 (2000)

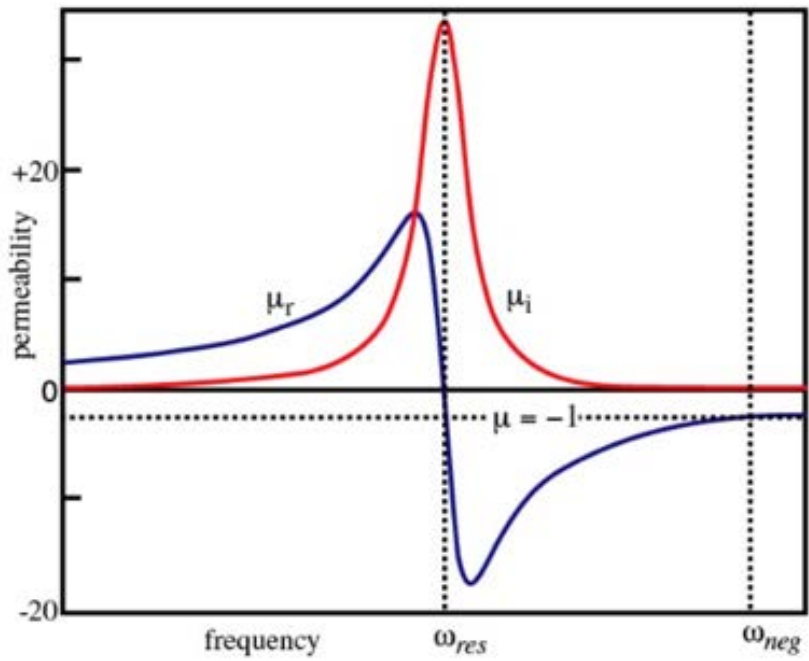


Le circuit RLC



Th
 M_d
abo

As
ciat
inci



$$\frac{d^2q}{dt^2} + \frac{R}{L} \frac{dq}{dt} + \frac{1}{LC} q = 0$$

$$\gamma = \frac{R}{L}; \quad \omega_0^2 = \frac{1}{LC}$$

intérêt des métamatériaux :

Permettent :

- de choisir l'indice du milieu et sa perméabilité magnétique
- de rendre une surface non réfléchissante pour tout indice
- de créer des indices négatifs
- de créer des indices énormes
- de créer de fortes anisotropies
- de rendre invisible

Les métamatériaux

- pour rendre un indice n très élevé

Metamaterial breaks refraction record

Feb 16, 2011 [1 comment](#)



Record-breaking metamaterial

Researchers in Korea have created a new metamaterial with the most extreme positive index of refraction yet – a whopping 38.6. The metamaterial operates at terahertz frequencies and the team believes that it could find use in a number of applications including high-resolution imaging.

A terahertz metamaterial with unnaturally high refractive index

Muhan Choi^{1*}, Seung Hoon Lee^{2*}, Yushin Kim¹, Seung Beom Kang², Jonghwa Shin¹, Min Hwan Kwak², Kwang-Young Kang², Yong-Hee Lee¹, Namkyoo Park¹ & Bumki Min¹

Controlling the electromagnetic properties of materials, going beyond the limit that is attainable with naturally existing substances, has become a reality with the advent of metamaterials^{1–3}. The range of various structured artificial 'atoms' has promised a vast variety of otherwise unexpected physical phenomena^{4–17}, among which the experimental realization of a negative refractive index has been one of the main foci thus far. Expanding the refractive index into a high positive regime will complete the spectrum of achievable refractive index and provide more design flexibility for transformation optics^{18–24}. Naturally existing transparent materials possess small positive indices of refraction, except for a few semiconductors and insulators, such as lead sulphide or strontium titanate, that exhibit a rather high peak refractive index at mid- and far-infrared frequencies¹⁸. Previous approaches using metamaterials were not successful in realizing broadband high refractive indices^{25–27}. A broadband high-refractive-index metamaterial structure was theoretically investigated only recently²², but the proposed structure does not lend itself to easy implementation. Here we demonstrate that a broadband, extremely high index of refraction can be realized from large-area, free-standing, flexible terahertz metamaterials composed of strongly coupled unit cells. By drastically increasing the effective permittivity through strong capacitive coupling and decreasing the diamagnetic response with a thin metallic structure in the unit cell, a peak refractive index of 38.6 along with a low-frequency quasi-static value of over 20 were experimentally realized for a single-layer terahertz metamaterial, while maintaining low losses. As a natural extension of these single-layer metamaterials, we fabricated quasi-three-dimensional high-refractive-index metamaterials, and obtained a maximum bulk refractive index of 33.2 along with a value of around 8 at the quasi-static limit.

According to the Maxwellian macroscopic description, the effective relative permittivity of an artificial medium can be written as $\epsilon = 1 + (P/\epsilon_0 E)$ and the effective relative permeability can be defined by $\mu = 1 + (M/H)$, where E , H , P and M denote electric field, magnetizing field, polarization and magnetization, respectively. In order to tailor the value of the refractive index by controlling the degree of polarization and magnetization, we used a strongly coupled, thin T-shaped metallic patch to maximize the effective permittivity ϵ while suppressing the diamagnetic effect. A similar T-shaped patch structure in the weakly and moderately coupled regimes has been used to provide the index variations required for broadband ground-plane cloaking in the microwave frequency bands¹³.

The basic building block (single-layer unit cell) of the proposed high-refractive-index terahertz metamaterial is shown in Fig. 1a, together with the polarization of an incident terahertz wave. (In Supplementary Information we describe the polarization dependence of this system. We note that two-dimensionally isotropic high-index

metamaterials can be designed; the results are given in Supplementary Information.) Here, the substrate is made from a dielectric material and the thin T-shaped metallic patch is embedded symmetrically in the substrate. Throughout this work, the substrate was implemented with polyimide (real part of the refractive index n , $Re(n)$, is 1.8) and the metals used to construct the metamaterials were gold (on chromium) or aluminium (see Methods Summary). Optical micrographs of the fabricated large-area (2×2 cm), free-standing, flexible metamaterials are shown in Fig. 1b. Precise alignment between stacked metamaterial layers has been achieved, as can be confirmed by the higher-magnification microscope images shown in the upper insets of Fig. 1b. As the substrate is made from flexible polyimide, the fabricated metamaterials are also extremely flexible, and the samples are perfectly free-standing (lower inset of Fig. 1b).

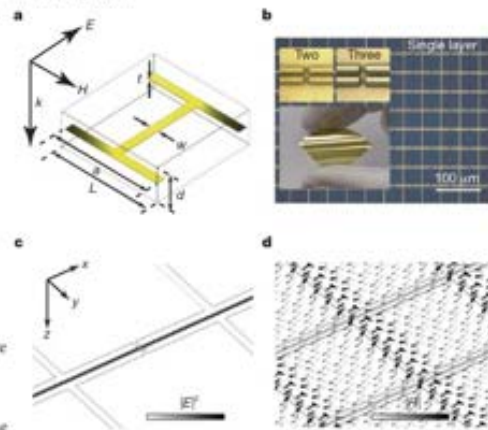


Figure 1 | Schematic view of the high-index metamaterials and images of the fabricated metamaterials. **a**, Unit cell structure of the high-index metamaterial, made of a thin T-shaped metallic patch symmetrically embedded in a dielectric material. The incident terahertz wave is directed downwards, with the polarization of the wave indicated by the arrows. **b**, Optical micrograph of fabricated single-layer metamaterial. Top insets, higher-magnification micrographs, showing the alignment of constituent metamaterial layers for double- and triple-layer metamaterials. Bottom inset, photograph of a flexibility test for the fabricated metamaterials. **c**, Saturated electric field (at 0.33 THz) for a single-layer metamaterial with a unit cell of $L = 60 \mu\text{m}$, $a = 58.8 \mu\text{m}$, $d = 2.45 \mu\text{m}$, and $w = 3 \mu\text{m}$. Shading indicates modulus of field to the power two. **d**, Vector plot of the magnetic field (at 0.33 THz) in the unit cells. Shading indicates modulus of field.

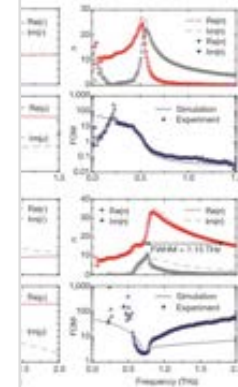


Figure 2 | Effective permittivity, permeability, refractive index of metamaterials. **a**, Effective permittivity (ϵ_{eff} , bottom left) extracted from the characterization of unit cell. Experimentally obtained complex top right, along with the corresponding numerical simulation (black line) from the 5-parameter retrieval method. Bottom of inset (FOM) together with the numerically simulated parameters of the unit cell are the same as those used for Fig. 1c and d. In the plots, data points and solid and numerical data, respectively. **b**, As a by-product, the gap width g is set to $1.5 \mu\text{m}$, the length of w of metallic structure is $3 \mu\text{m}$, and the thickness t of an additional polyimide layer of $\sim 0.8 \mu\text{m}$ on the fabricated metamaterials.

the enhancement of the effective refractive index spectroscopy²⁸ (THz-TDS) was performed at 0.1–2 THz. All the samples were prepared by micro/nano-fabrication processes (see visible extraction of the complex refractive indices through an iterative algorithm considering the sample was applied to the field H_z). Next, the complex refractive indices DS measurements were compared with the values from the 5-parameter extraction, considering the uncertainties in the material modulation and the errors in the gap-width iteratively acquired complex refractive index n with the simulated refractive index. From single-layer metamaterial, a peak refractive index was observed, with a value of $n = 11.18$ at less associated with the single-layer metamaterial figure of merit (FOM) $\text{Re}(n)/\text{Im}(n)$; calculated values of FOM are plotted in the box. For most frequency ranges, especially in the electric resonance, the FOM stays above 100.

By raising the refractive index has been extended for single-layer metamaterials, further into an investigation into three-dimensional

formation of the gap width, along with simulated optical spectra ($\sim 80 \text{ nm}$) high index material used to define the metallic patch in the sample. **c**, Frequency dependent effective permittivities with varying gap widths. **d**, respectively. Bottom, frequency of peak loss of the gap width, along with simulated optical spectra ($\sim 80 \text{ nm}$) high index material used to define the metallic patch in the sample. **e**, Frequency dependent effective permittivities with varying gap widths.

Publishers Limited. All rights reserved

of the slab is maximized and f_0 denotes the frequency of the Bloch modes where $p = 0, \dots, N - 1$, is a sensitive function of the gap metamaterials. Bearing this in mind of a physically achievable semantically approach this limit, metamaterials having gap widths w (measured and numerically) function of the gap width (top quasi-static limit, bottom panel, refractive indices obtained from an asymptotic formula and its fit index is 26.8 at the quasi-static limit) for the sample with 80 nm gap value was greater than 20 at peak; Fig 4b and c). In the weakly g between unit cells is negligible approximated as

$$\epsilon_{\text{eff}} = \frac{\epsilon_0 E E}{2 \sqrt{3} d} (1 - \frac{d^2}{L^2})$$

parameters. However, as the gap size to coupling between unit cells index of refraction is drastically vertical to the inverse $(1 - f_0^2/f_c^2)^{-1/2} (1 - f_0^2/f_c^2)^{-1/2}$, so the

at 180 °C in a convection oven for 30 min; curing process of the polyimide layers was ended quartz tube furnace under an inert acid into a fully aromatic and insoluble ZnO/P2O5, AZ Electronic Materials) was removed photolithography. AuCr (90 nm) served as T-shaped array structure via the inside coating and coating processes, single- and multi-layered metamaterials on the silicon; the above single-layer process until the N was stacked. Finally, the flexible terahertz slab off the metamaterial layers from the N the microscale gap metamaterials were as positive, and 3D printed metamaterial. Nano-gap flexible substrate N same process for the microscale gap metamaterial process, which used electron beam lithography. Thin aluminum film was evaporated onto and patterned as a connected T-shaped shape. Etching windows for 80-nm gaps were lithography. As T-shaped aluminum beams etching using an electron beam resist mask removing the residual resist and after the gap terahertz metamaterials were fabricated on

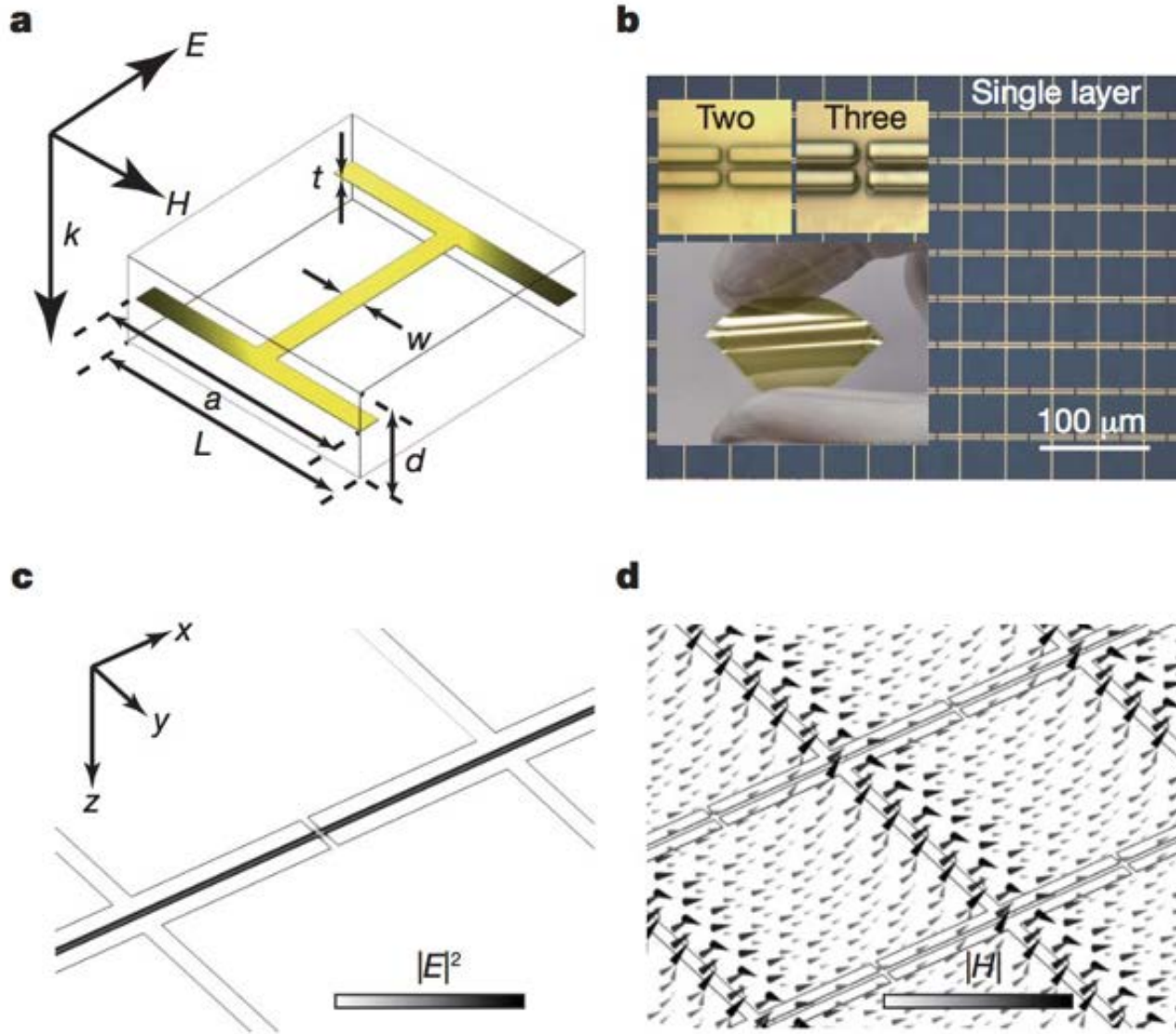
under 2012. **1** of publications with author(s) negative **1**, 2012-2014 (1944). **1**, D. J. & Bower, W. J. Magnetism from **1** (phenomena, IEEE Trans, Microwave Theory

17 FEBRUARY 2011 | VOL 470 | NATURE | 349

¹Department of Mechanical Engineering, Korea Advanced Institute of Science and Technology (KAIST), Daejeon 305-701, South Korea. ²Convergence Components and Materials Research Laboratory, Electronics and Telecommunications Research Institute (ETRI), Daejeon 305-700, South Korea. ³Department of Physics, Korea Advanced Institute of Science and Technology (KAIST), Daejeon 305-701, South Korea. ⁴School of Electrical Engineering and Computer Science, Seoul National University, Seoul 151-744, South Korea. ⁵Present address: Convergence Components and Materials Research Laboratory, Electronics and Telecommunications Research Institute (ETRI), Daejeon 305-700, South Korea.

*These authors contributed equally to this work.

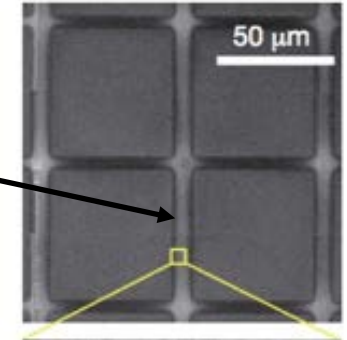
formes de I en or ou aluminium sur un polymère de 60 μm .



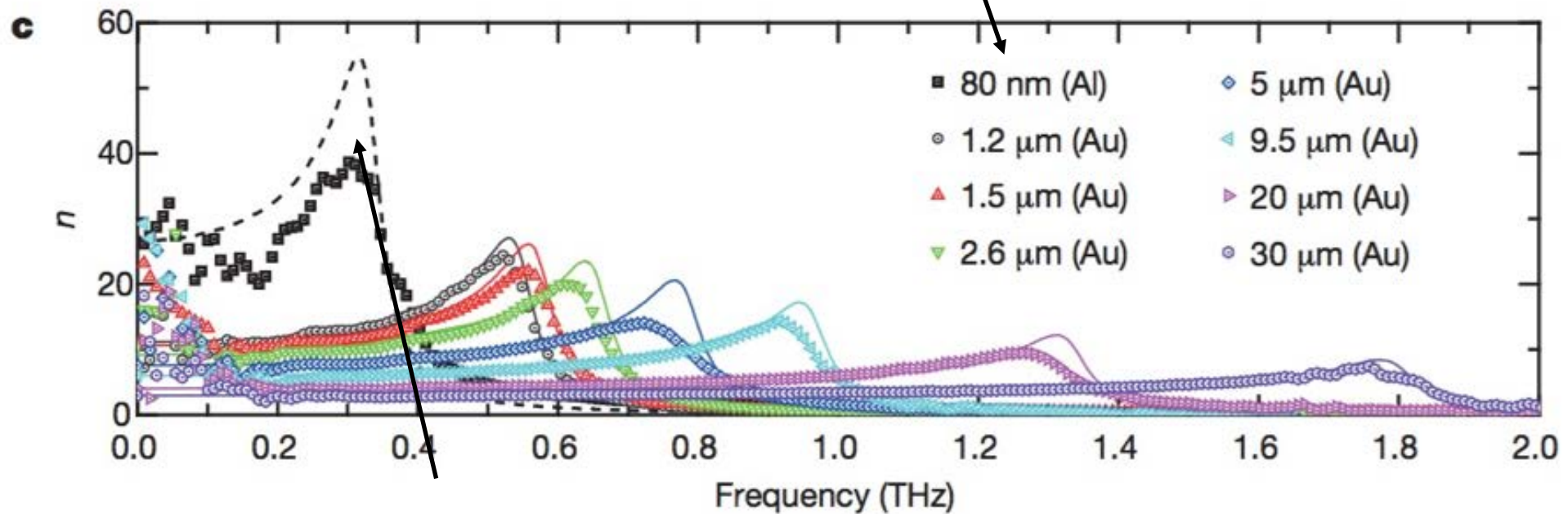
Le métal agit ici comme une capacité qui crée un champ électrique qui agit à son tour sur la lumière.

Figure 1 | Schematic view of the high-index metamaterials and images of the fabricated metamaterials. a, Unit cell structure of the high-index metamaterial, made of a thin 'T'-shaped metallic patch symmetrically embedded in a dielectric material. The incident terahertz wave is directed downwards with the polarization of the wave indicated by the arrows.

indice n pour différentes fabrications :
on peut aller jusqu'à $n=50$ à 60 !



taille du trou
entre les éléments



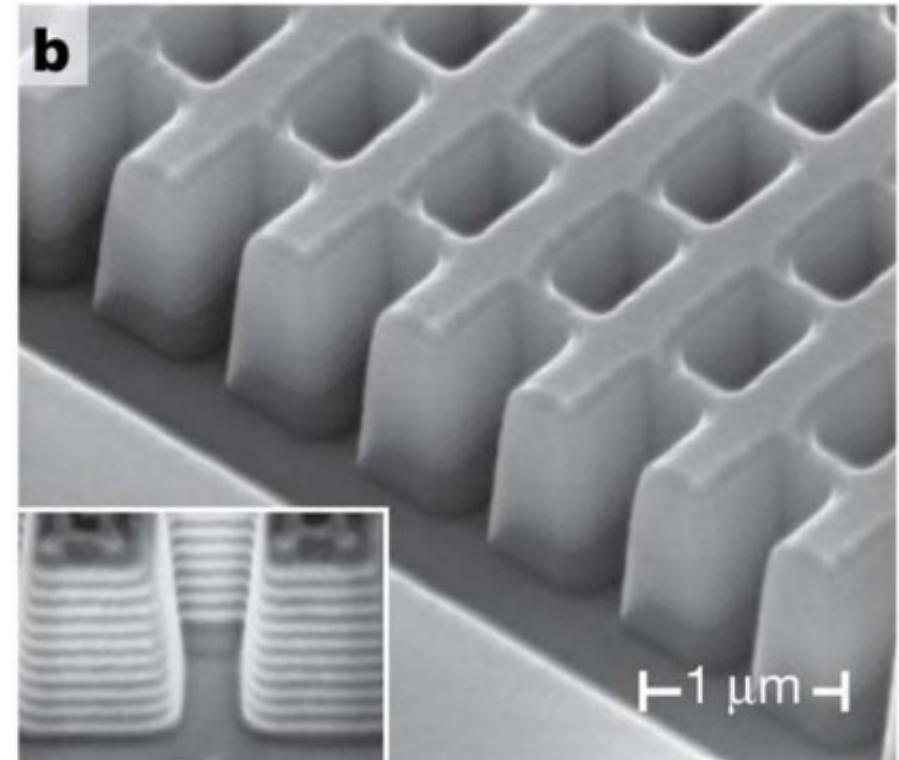
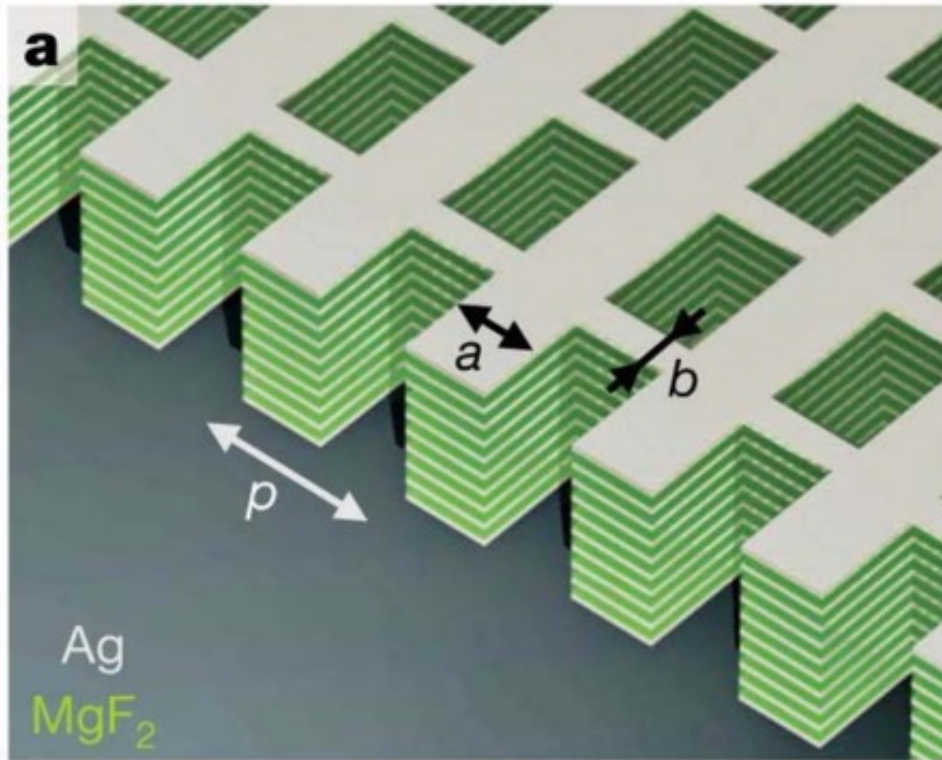
38.6 à 0.3 THz

Les métamatériaux

- pour rendre un indice n élevé
- pour rendre un indice n négatif

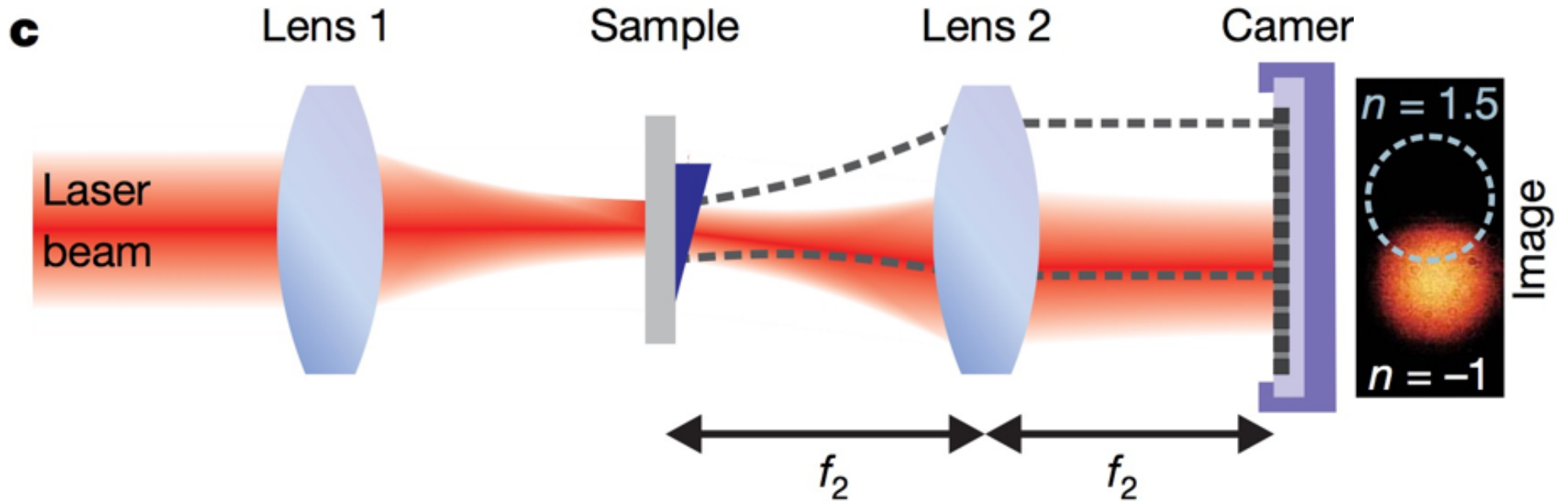
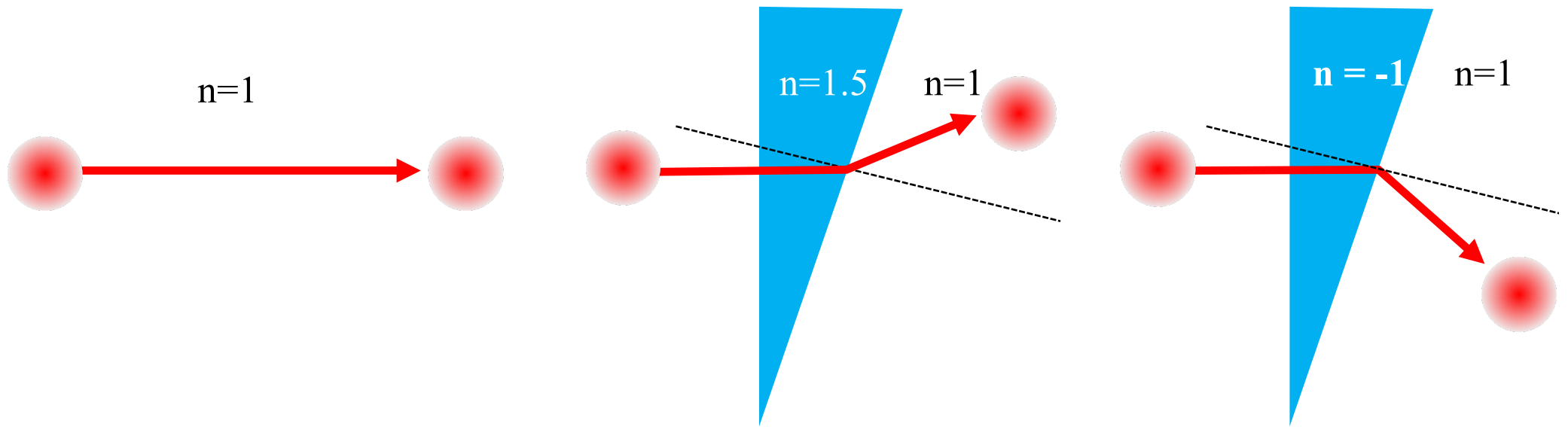
Three-dimensional optical metamaterial with a negative refractive index

Jason Valentine^{1*}, Shuang Zhang^{1*}, Thomas Zentgraf^{1*}, Erick Ulin-Avila¹, Dentcho A. Genov¹, Guy Bartal¹ & Xiang Zhang^{1,2}

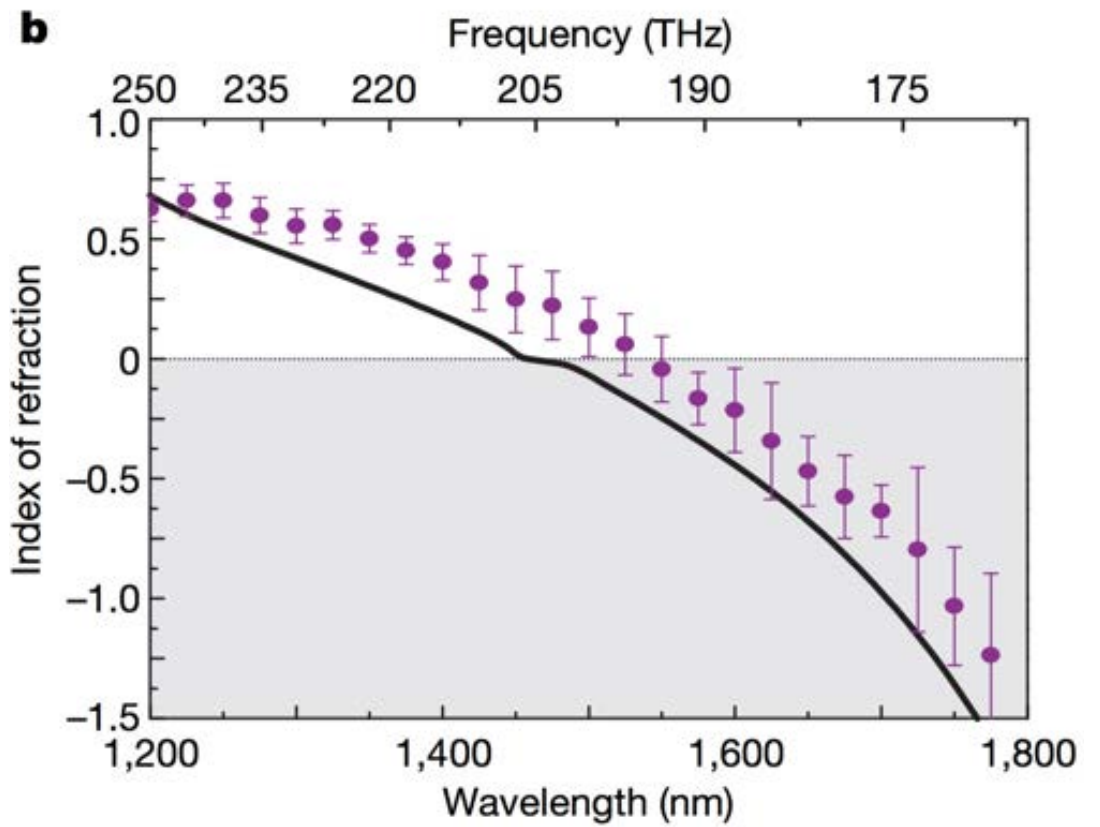
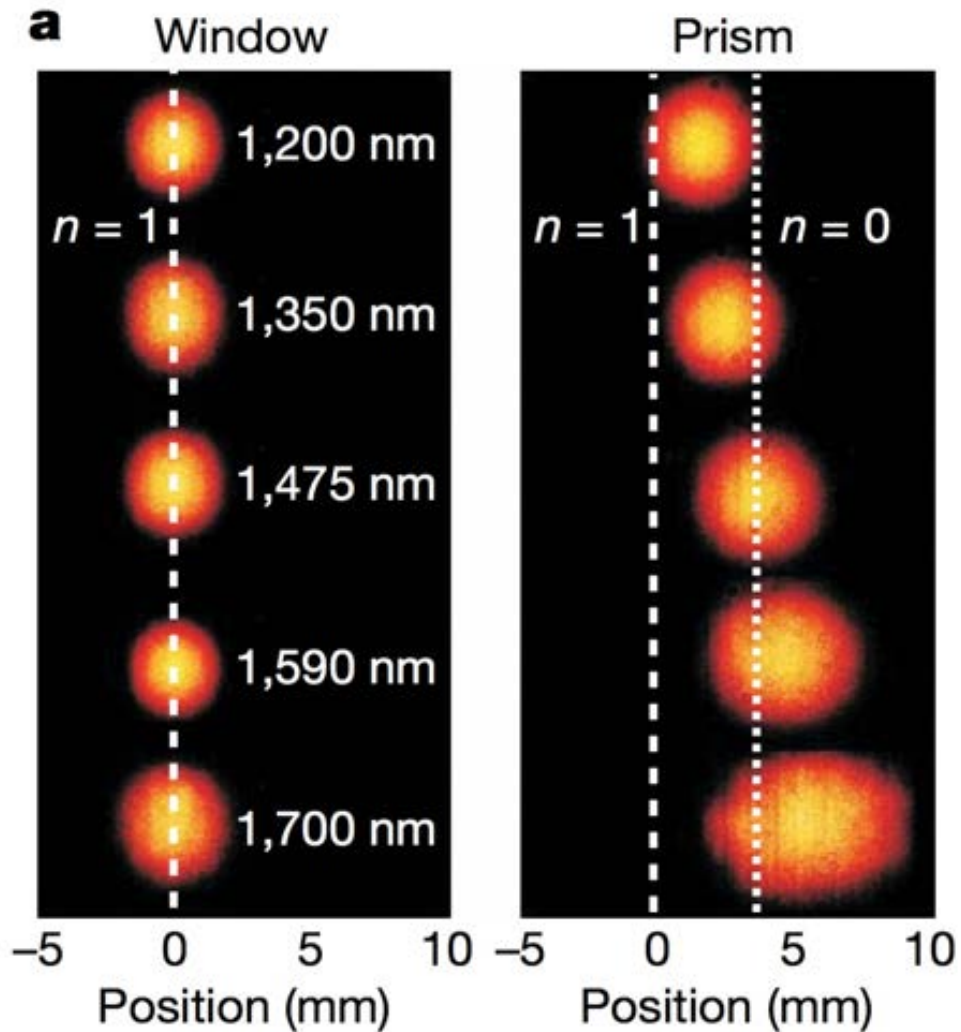


structure en filet de pêche : alternance de couches d'argent de 30nm et de MgF₂ de 50nm
→ couplage de circuits résonants LC d'où effet magneto-inductif équivalent à un indice négatif

Rendre l'indice négatif



variation de n avec la longueur d'onde de la lumière utilisée

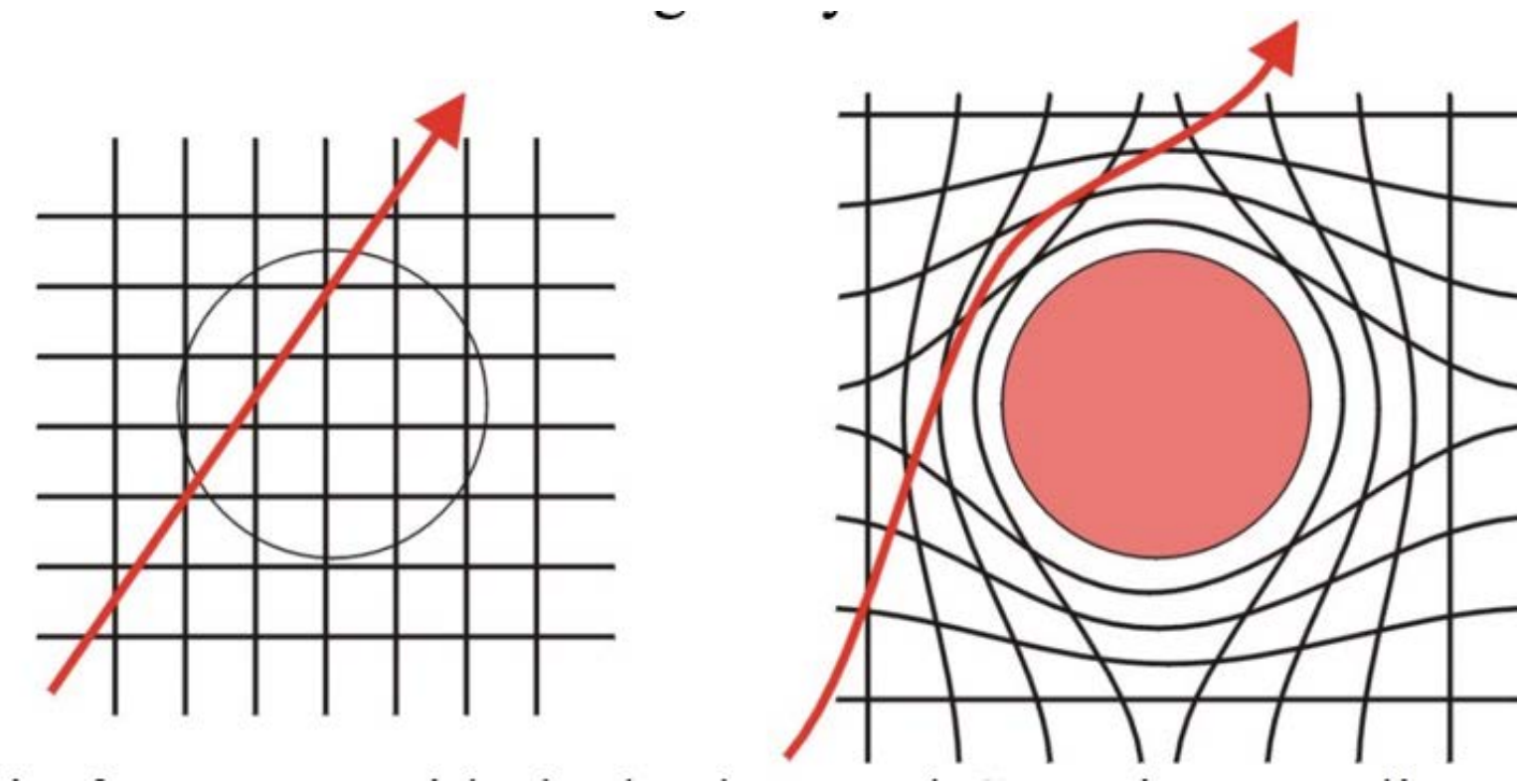


Les métamatériaux

- pour rendre un indice n élevé
- pour rendre un indice n négatif
- **pour rendre invisible**

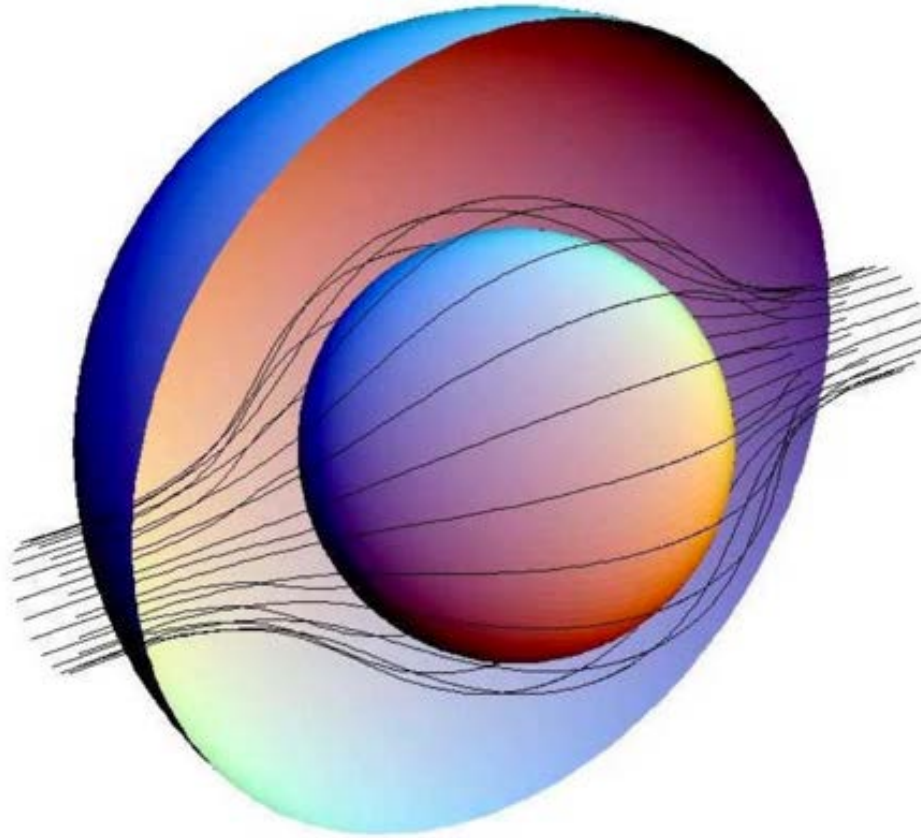
l'invisibilité

Construire un matériau qui a l'indice permettant de dévier exactement la lumière comme si l'objet n'existait pas :



l'invisibilité

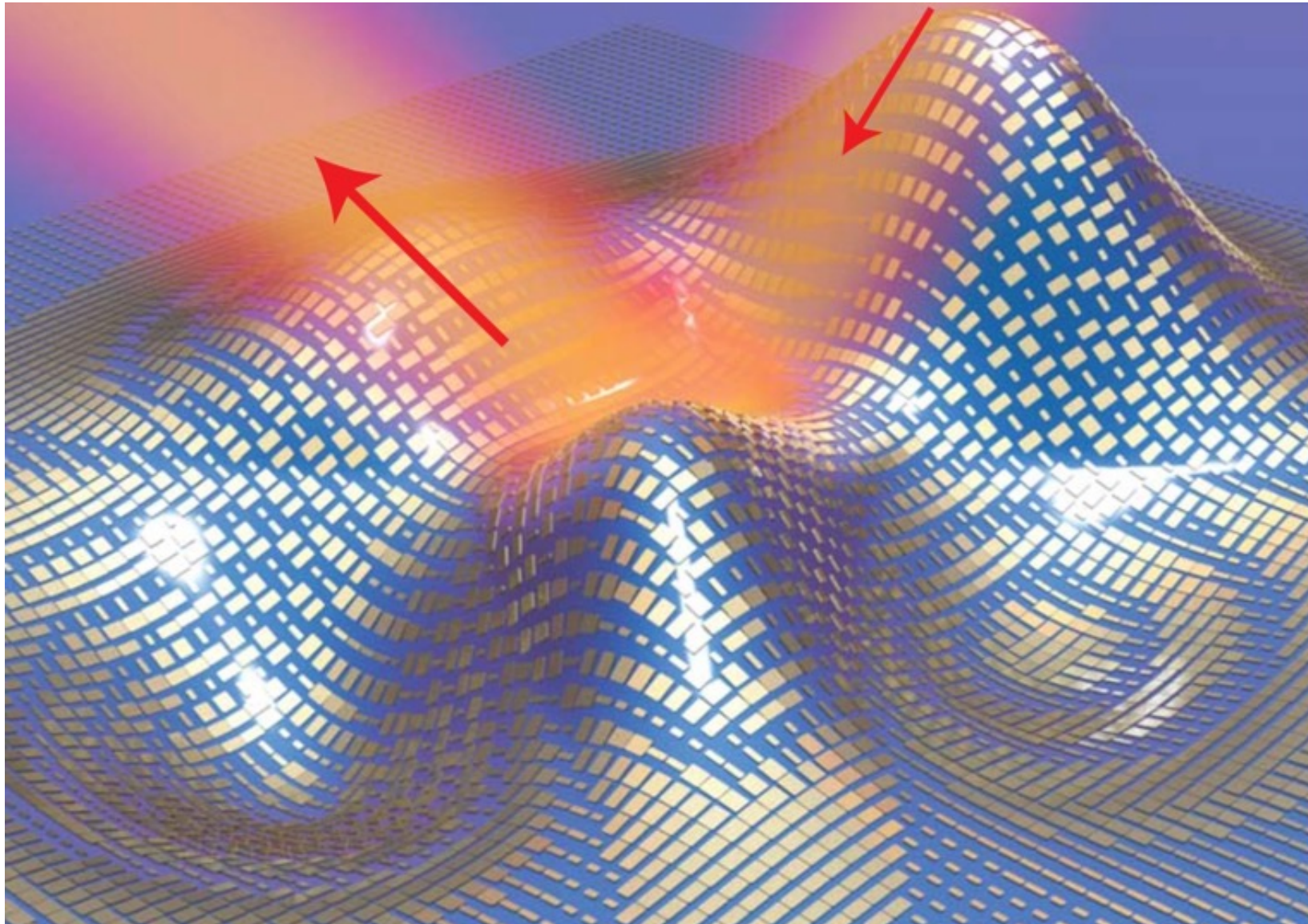
Construire un matériau qui a l'indice permettant de dévier exactement la lumière comme si l'objet n'existait pas :



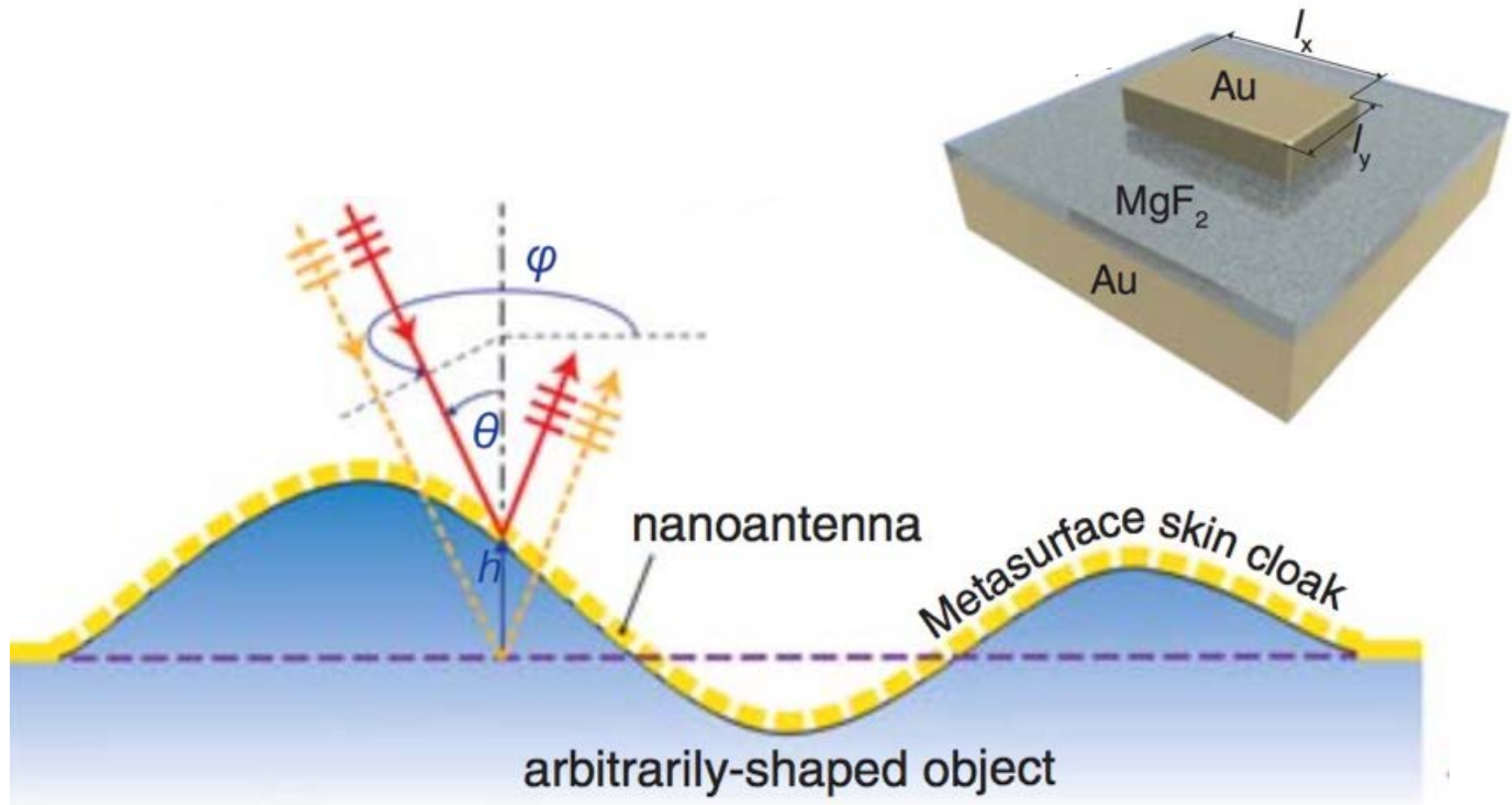
An ultrathin invisibility skin cloak for visible light

Xingjie Ni,^{1*} Zi Jing Wong,^{1*} Michael Mrejen,¹ Yuan Wang,^{1,2} Xiang Zhang^{1,2,3†}

Science 2015

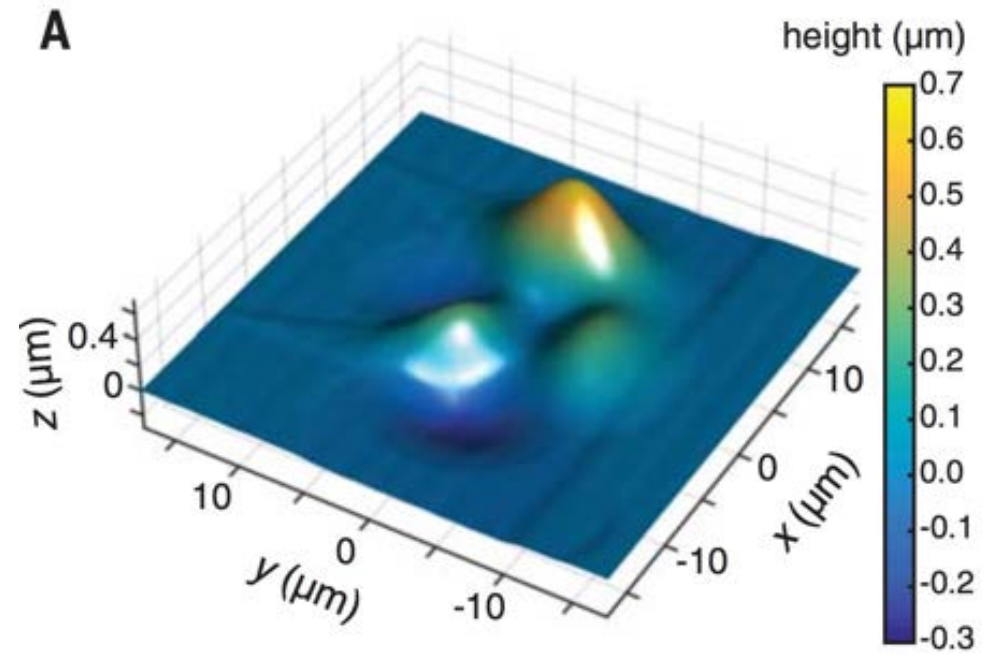


métasurface ultrafine (80nm) composée de nano-antennes d'or

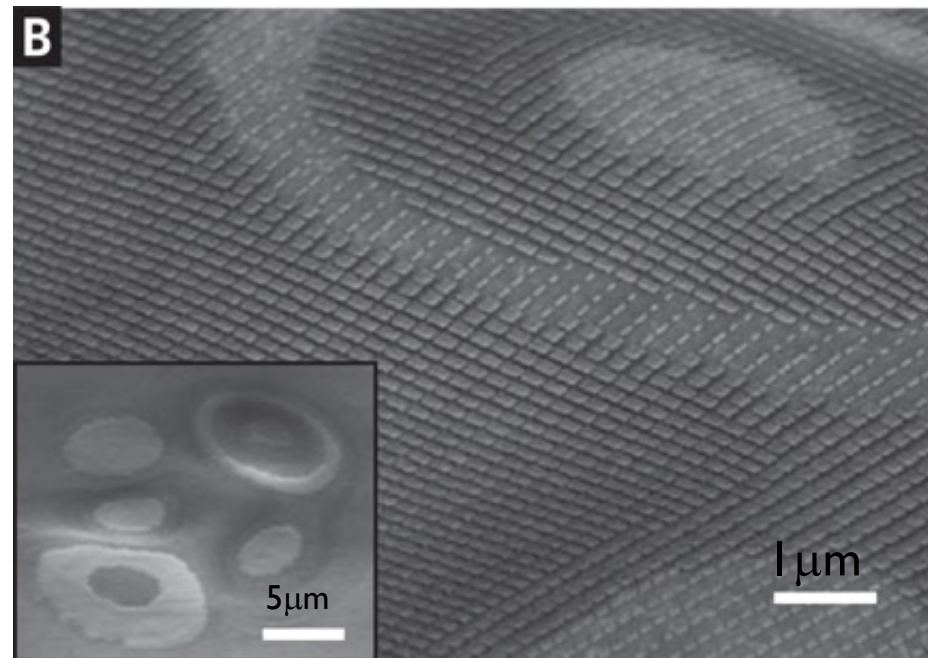


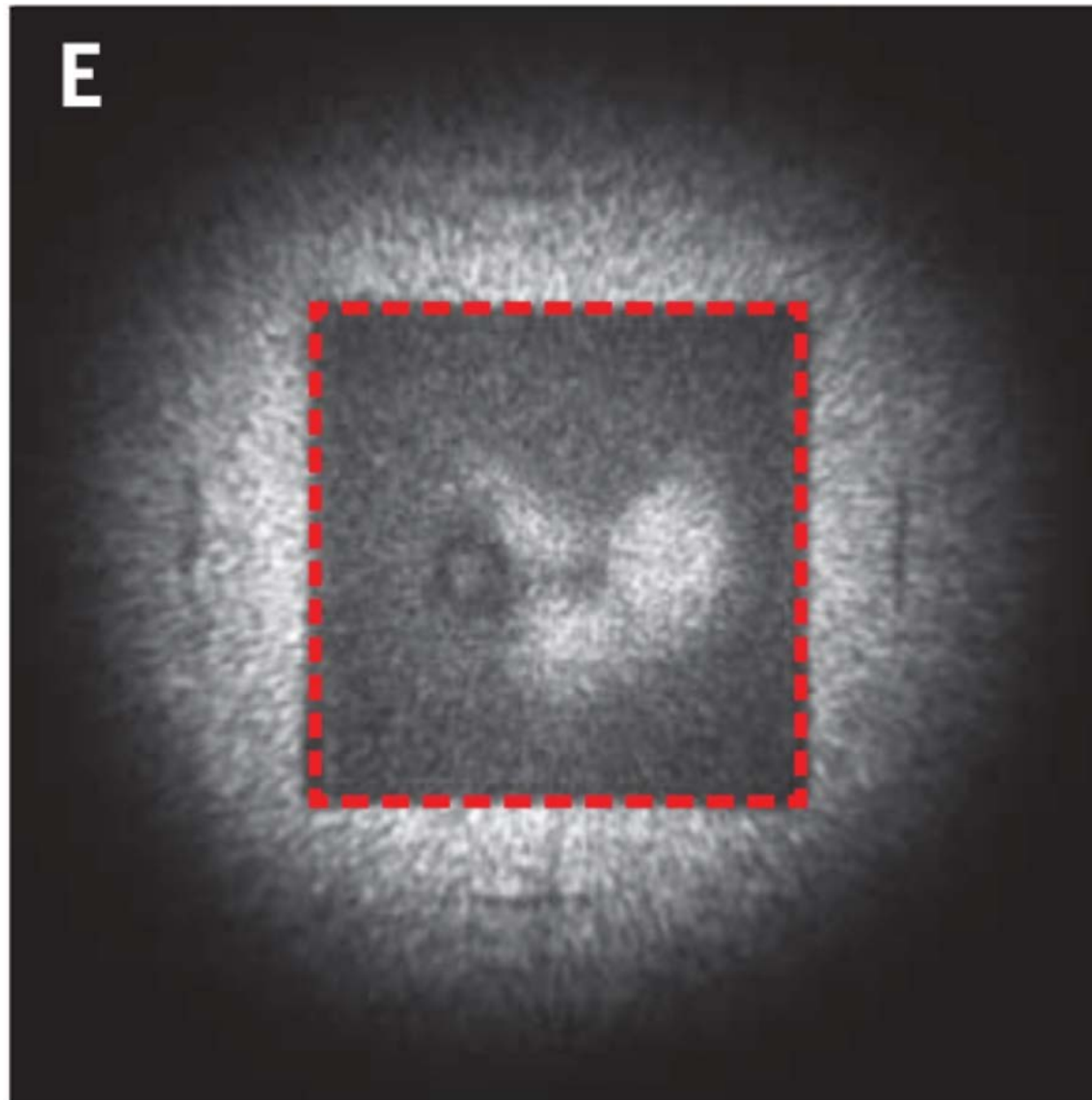
chaque nano-antenne produit via l'ajustement de sa taille (l_x, l_y) un déphasage pour rattraper l'effet de la hauteur de matériau h : émission comme si il s'agissait d'un miroir plan (au niveau violet)

l'objet de départ

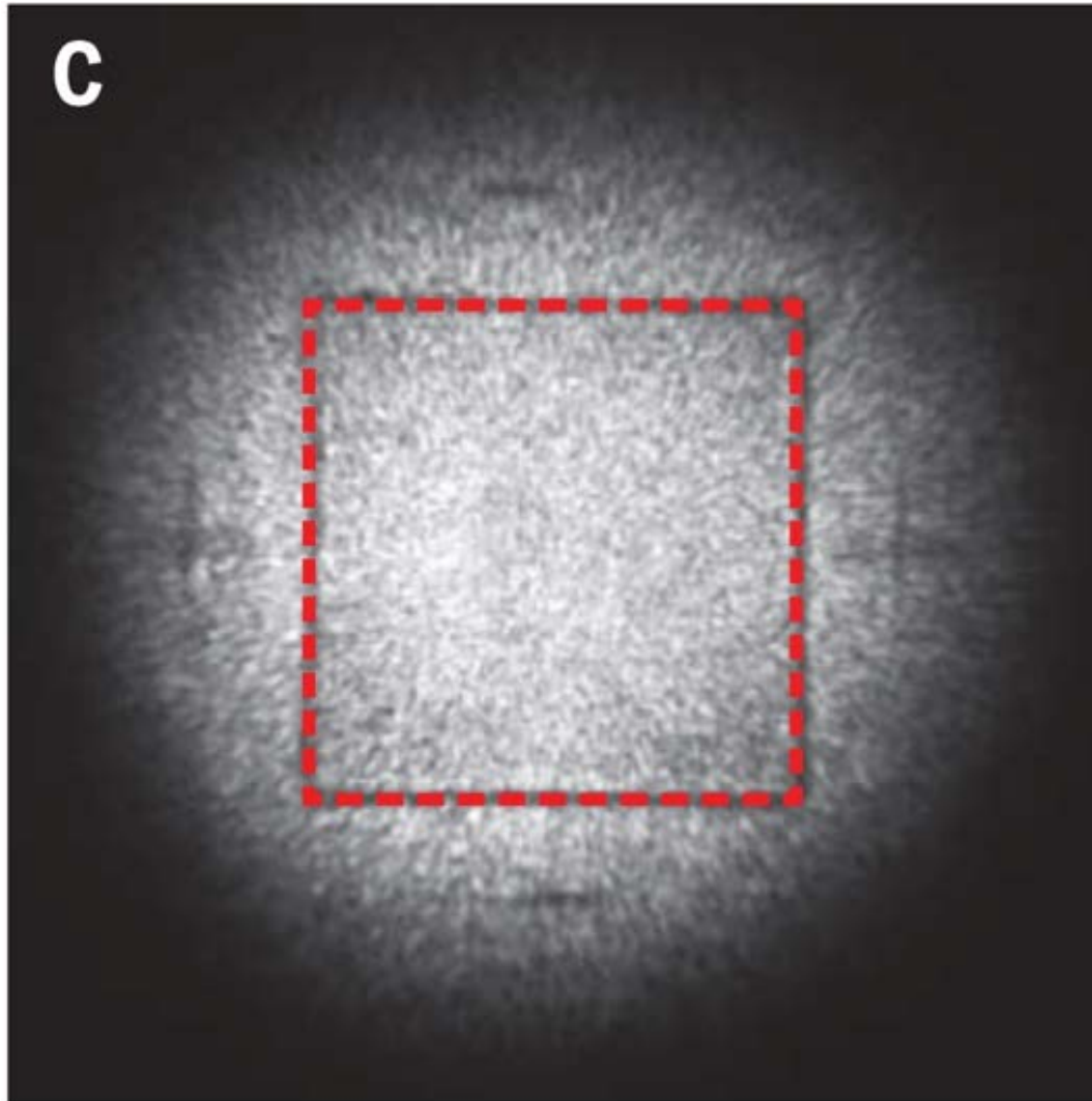


l'objet recouvert
des nano-antennes





$\lambda=730\text{nm}$



$\lambda=730\text{nm}$

→ ça fait disparaître le relief

Limitations :

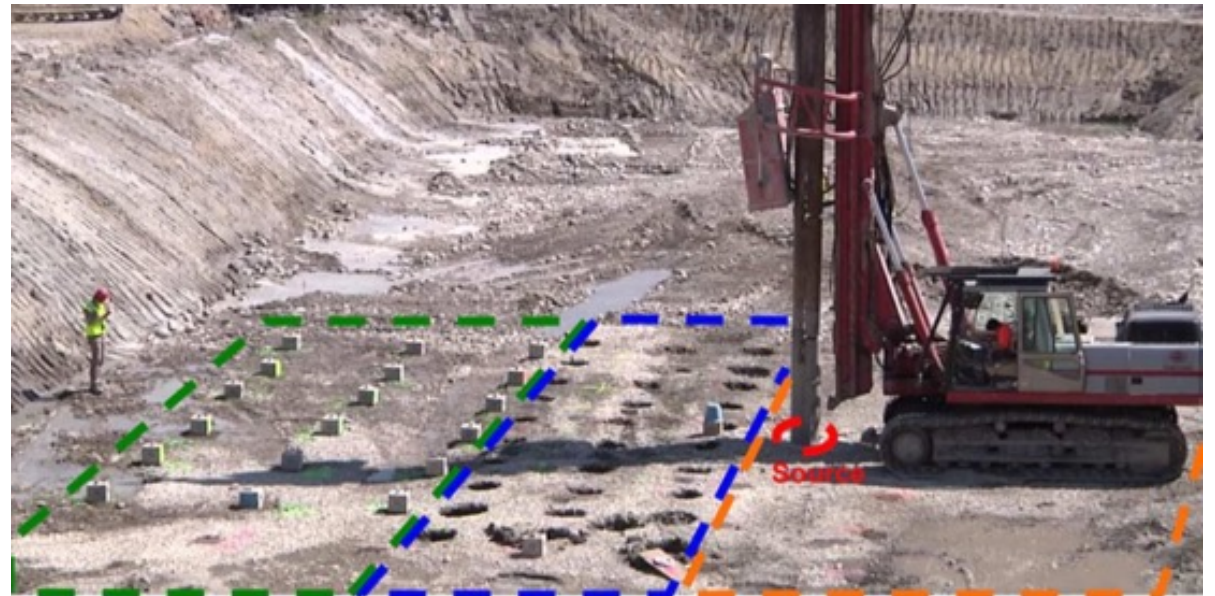
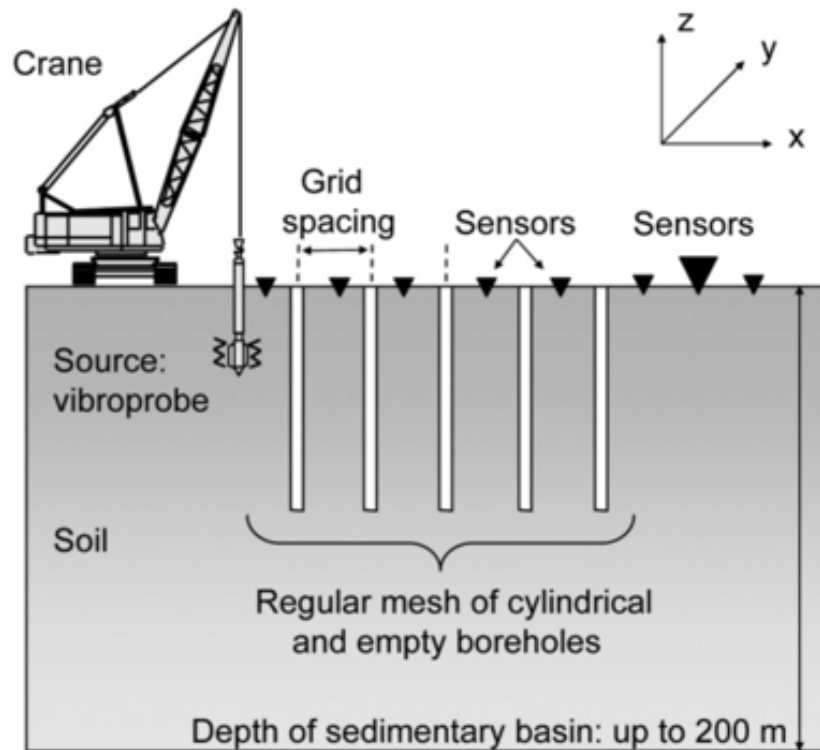
- design des antennes adapté au relief donc on ne peut pas bouger
- Plage de fréquence limitée
- Objet à cacher pas trop gros sinon impossible de cacher son ombre

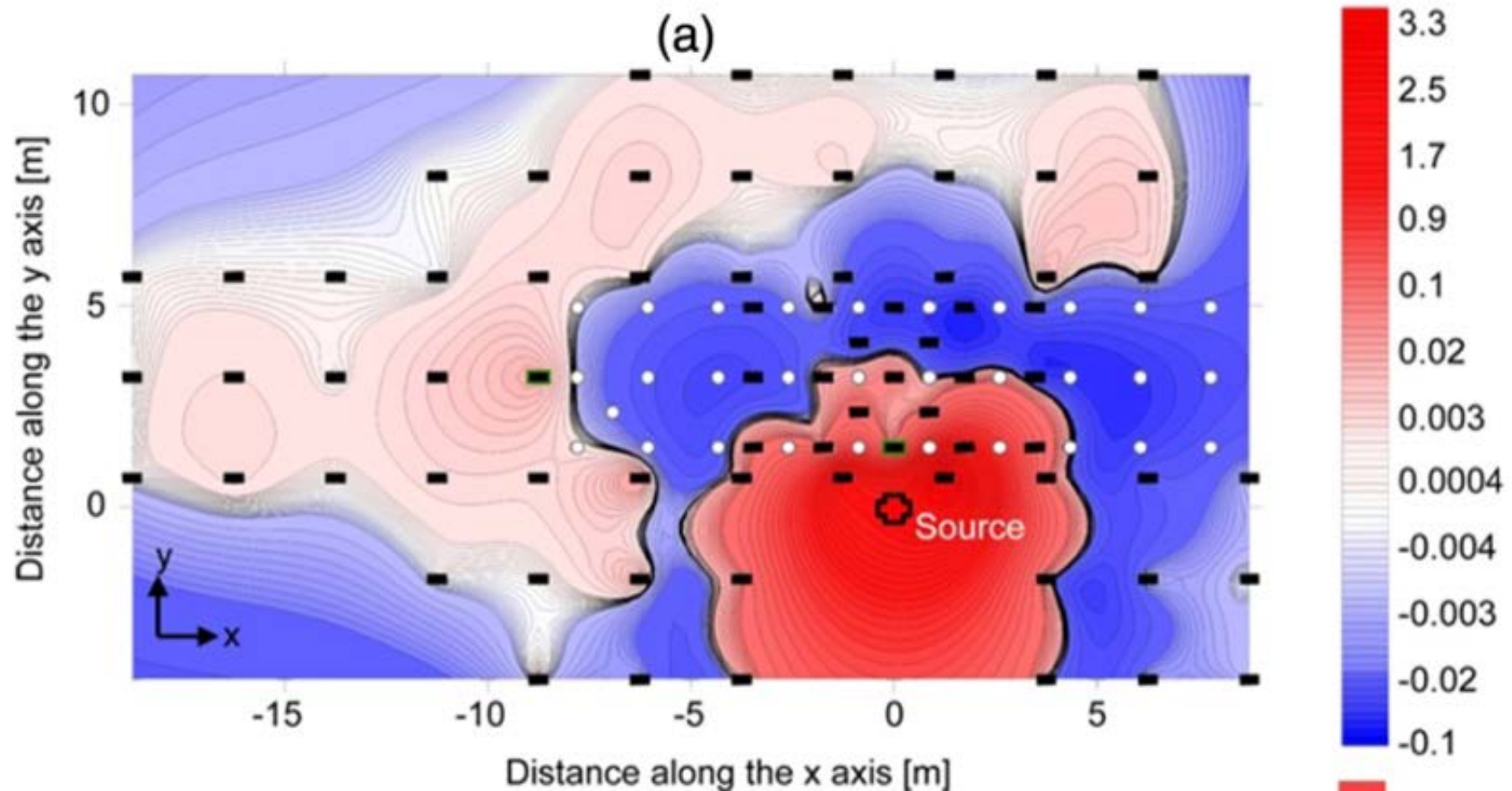
applications possibles

- invisibilité
- ralentir la lumière → aller vers du stockage d'information
- guider la lumière en fabriquant un n qui varie dans l'espace sur mesure
- créer des lentilles parfaites
- créer des absorbeurs de lumière parfaits (trous noirs)

s'inspirer des métamatériaux : pour les ondes sismiques

un réseau de trous périodiques
bloque l'onde sismique





Brulé PRL 2014

différence entre avec et sans les trous:
le seisme est confiné près de la source
et stoppé dans la zone bleue

s'inspirer des métamatériaux :
pour les ondes acoustiques

pour les guider, les absorber,
les rendre invisibles, créer des lentilles...

Problème : grande longueur d'onde

Astuce : des composants astucieux pour travailler à des
longueurs d'onde 10 à 100 fois plus grandes



mech.kuleuven.be

résumé

Les lois de Descartes sont bien vérifiées en optique géométrique.

Méta-matériaux : structures périodiques de circuits électriques qui modifient les lois habituelles de l'optique et permettent de choisir sur mesure l'indice n (négatif, variable, positif, élevé...).

Intérêt en optique pour manipuler la lumière mais aussi dans tous les domaines avec des ondes (acoustique, mécanique...)

Perspectives : imaginer de nouveaux matériaux affectant les lois habituelles de l'optique pour les télécommunications, les nanotechnologies, ou contourner les limitations habituelles de l'optique géométrique (invisibilité...)